

# The Overhead Line Sag Dependence on Weather Parameters and Line Current

---

Elisabeth Lindberg

# Abstract

## The overhead line sag dependence on weather parameters and line current

*Elisabeth Lindberg*

As the demand for energy increases, as well as the demand for renewable energy, Vattenfall, as network owner, receives many requests to connect new wind power to the grid. The limiting factor for how much wind power that can be connected to the grid is in this case the maximum current capacity of the overhead lines that is based on a line temperature limit. The temperature limit is set to ensure a safety distance between the lines and the ground.

This master thesis project is a part of a research project at Vattenfall Research and Development that is examining the possibilities of increasing the allowed current on overhead lines in order to be able to connect more wind power to the existing network. Measured data from two overhead lines in southern Sweden is analyzed and the internal relations between the measured parameters are examined. The measured parameters are overhead line sag, line temperature, ambient temperature, solar radiation, wind speed and line current.

The results indicate that there is a big load margin that could be utilized to increase the maximum current as long as further work could show that low winds at line height correlates with low wind at nacelle height. The results show that the sag versus line temperature is approximately linear within the measured temperature range. This means that a real-time-monitoring system measuring the line temperature should give adequate knowledge of the line position to ensure the safety distance. A model for the line temperature as a function of insolation, current, ambient temperature and wind speed has been estimated for one of the lines. Simulations show that a sudden increase in current at a worst-case scenario would give the operators about ten minutes to react before the line reaches the temperature limit.

Keywords: Overhead lines, dynamic rating, real-time monitoring, conductor temperature model, sag

*Department of Information Technology, Uppsala University, Box 337, SE- 751 05  
Uppsala  
ISSN 1401-5765*

# Referat

## Beroendet av väderparametrar och ström hos nedhäng på luftledningar

*Elisabeth Lindberg*

Då energibehovet i samhället ökar samt intresset för förnyelsebar energi har Vattenfall börjat få väldigt många förfrågningar om nya vindkraftanläggningar som vill ansluta till Vattenfalls nät. Den begränsande faktorn för hur mycket vindkraft som kan anslutas till nätet blir i detta fall den maximalt tillåtna strömmen i luftledningarna, vilken baseras på en maximal tillåten temperatur på ledningen. Denna maxgräns är satt så att den garanterar att säkerhetsavståndet mellan ledningen och marken inte blir för litet.

Det här examensarbetet är en del i ett forskningsprojekt på Vattenfall Research and Development som undersöker möjligheten att öka den maximalt tillåtna strömmen i luftledningar för att kunna ansluta mer vindkraft till nätet. Mätdata från två luftledningar i södra Sverige har analyserats och sambanden mellan de mätta parametrarna har studerats. De mätta parametrarna är linans nedhäng, lintemperatur, lufttemperatur, solinstrålning, vindhastighet och ström.

Resultaten tyder på att det finns en stor marginal som skulle kunna utnyttjas för att öka den maximalt tillåtna strömmen i linan, under förutsättning att även en korrelation mellan låg vind på lin-höjd och låg vind på vindkraftverks-höjd kan påvisas i fortsatta studier. Resultaten visar att linans nedhäng har ett approximativt linjärt förhållande till lintemperaturen. Detta betyder att ett realtidsövervakningssystem med lintemperaturmätning skulle kunna bestämma linans position med tillräcklig noggrannhet för att kunna garantera att säkerhetsavståndet bibehålles. En modell för lintemperaturen som funktion av ström, solinstrålning, lufttemperatur och vindhastighet har anpassats för en av linorna. Simuleringar har visat att vid en plötslig strömökning vid ett värsta tänkbara scenario skulle operatörerna ha ungefär tio minuter på sig att reagera innan linan når temperaturgränsen.

Nyckelord: Luftledningar, dynamisk rating, realtidsövervakning, lintemperaturmodell, nedhäng

*Institutionen för informationsteknologi, Uppsala universitet, Box 337, SE- 751 05  
Uppsala  
ISSN 1401-5765*

## Preface

This master thesis project was performed at Vattenfall R&D in Råcksta, Stockholm, from November 2010 to June 2011, within the Master of Science program in Aquatic and Environmental Engineering at Uppsala University. Supervisors at Vattenfall were Lovisa Stenberg and Urban Axelsson. Subject reviewer was Bengt Carlsson, Department of information technology at Uppsala University and examiner was Allan Rodhe, Department of earth sciences at Uppsala University. This master thesis has been a part of the research project Wind cooled OH lines at Vattenfall.

First I would like to thank Vattenfall R&D for giving me this opportunity of working with this interesting project. Many thanks to Urban Axelsson and Lovisa Stenberg for their commitment and guidance during this project. Their support has been of great importance for me and this project. Thanks to Bengt Carlsson for ideas and support with the line temperature modelling. Thanks to Stefan Lindström for helping me with the sag modelling. Thanks to Elisabeth Larsson, Martin Tillenius and Marcus Holm for their help with the Matlab programming. Thanks to Gunnar Erixon for guiding at the visit at the operation center in Trollhättan. Thanks to Tor Johansson and Arne Bergström especially for help with preparing the presentation and thanks to Peter Schelander for preparing weather data and for good advice.

Copyright © Elisabeth Lindberg and the Department of Information Technology,  
Uppsala University

UPTEC W 11 017, ISSN 1401-5765

Printed at the Department of Earth Sciences, Geotryckeriet, Uppsala University,  
Uppsala, 2011

# Populärvetenskaplig sammanfattning

## Beroendet av väderparametrar och ström hos nedhäng på luftledningar

*Elisabeth Lindberg*

Då energibehovet i samhället ökar samt intresset för förnyelsebar energi har Vattenfall börjat få väldigt många förfrågningar av nya vindkraftanläggningar som vill ansluta till Vattenfalls nät. Längs vissa ledningssträckor på nätet räcker inte kapaciteten till för att vindkraftverken ska tillåtas att ansluta direkt till befintligt nät. Om kapaciteten på ledningarna överskrids blir ledningarna varmare än de är designade att klara av. Då blir nedhänget mellan ledningsstolparna stort och det säkerhetsavstånd som måste uppfyllas mellan ledningen och marken riskerar att bli för litet.

En lösning på detta problem skulle kunna vara att bygga ut kapaciteten genom att bygga nya ledningar. Problemet är att detta är en lång och dyr process som måste genomgå många instanser innan ledningar kan godkännas och byggas. En annan lösning är att se om kapaciteten i ledningarna egentligen är underskattade. Detta är grunden till det forskningsprojekt på Vattenfall Research and Development som detta examensarbete är en del av.

Kapaciteten i ledningarna begränsas alltså av ett minsta avstånd till mark som enligt lag måste upprätthållas. Avståndet till marken minskar när ledningen blir varm eftersom att materialet i linan utvidgas och linan blir längre. Temperaturen i linan bestäms av hur mycket ström som går i ledningen och av det omgivande vädret. Lufttemperatur, sol och vind har stor påverkan på linans temperatur. Eftersom att vindkraftverken som ska anslutas inte sätts igång för energiproduktion under en viss vindstyrka är tanken att belastningen på ledningarna inte kommer att ökas så länge vinden är svag och att när vinden är stark kommer den att kunna kyla av ledningen tillräckligt mycket för att jämna ut den uppvärmning som kommer av den ökade strömmen.

För att testa om detta är möjligt har man inom forskningsprojektet satt upp två stycken mätsystem på två ledningar i södra Sverige där man mäter vädret, strömmen, ledningens temperatur samt avståndet mellan ledningen och marken. Syftet med examensarbetet har varit att finna sambanden mellan de mätta parametrarna genom att analysera mätdata och att söka i litteratur.

Examensarbetet har lett till att en förenklad modell för ledningens temperatur som funktion av ström och väder har tagits fram samt en modell för storleken på ledningens nedhäng som funktion av ledningens temperatur på det spann där mätningarna har genomförts. Med modellen har man kunnat simulera ledningens

temperatur vid olika situationer. Med simuleringarna har man undersökt hur lång tid det skulle ta efter en kraftig strömökning i ledningarna under sämsta tänkbara väderförhållanden innan ledningens temperatur nått maxnivån. Detta motsvarar den tid en operatör i driftcentralen skulle ha på sig att agera vid en kraftigt uppmätt strömökning. Man har även undersökt hur stor påverkan de olika väderparametrarna har relativt varandra på temperaturökningen i ledningen och hur olika tjocklekar på linan påverkar reaktionstiden samt hur stor den verkliga outnyttjade kapaciteten har varit utgående från mätdata.

Resultaten tyder på att den outnyttjade kapaciteten i linan är stor (upp till dubbla kapaciteten), men inte förrän analys av de fortsatta mätningarna har gjorts går det att veta hur stor marginal som finns under den varmaste och kallaste delen av året. Det återstår även att undersöka om de tillfällen som ger lägst verklig kapacitet sammanfaller med låg vindhastighet vid högre höjd.

# Table of Contents

Page

|          |                                         |           |
|----------|-----------------------------------------|-----------|
| <b>1</b> | <b>INTRODUCTION</b>                     | <b>1</b>  |
| 1.1      | Purpose of the master thesis project    | 2         |
| 1.2      | About the report                        | 2         |
| <b>2</b> | <b>BACKGROUND</b>                       | <b>3</b>  |
| 2.1      | The Swedish grid                        | 3         |
| 2.2      | Overhead lines                          | 4         |
| 2.3      | ACSR conductors                         | 4         |
| 2.4      | The monitoring at operation centers     | 5         |
| <b>3</b> | <b>MEASUREMENTS</b>                     | <b>6</b>  |
| 3.1      | Two measurement sites                   | 6         |
| 3.1.1    | Site OL9                                | 6         |
| 3.1.2    | Site ZL8                                | 6         |
| 3.2      | Measurement system                      | 6         |
| 3.3      | Measurement data range                  | 9         |
| <b>4</b> | <b>THEORY</b>                           | <b>11</b> |
| 4.1      | Sag theory                              | 11        |
| 4.1.1    | Thermal elongation                      | 13        |
| 4.1.2    | Other line elongation causes            | 13        |
| 4.1.3    | Coupled spans                           | 14        |
| 4.2      | Conductor temperature model             | 15        |
| 4.2.1    | Current heating                         | 17        |
| 4.2.2    | Solar heating                           | 18        |
| 4.2.3    | Radiative cooling                       | 18        |
| 4.2.4    | Wind cooling                            | 20        |
| 4.3      | Thermal rating                          | 22        |
| 4.4      | Line uprating                           | 23        |
| 4.4.1    | Redefining weather conditions           | 23        |
| 4.4.2    | Dynamic Rating and real-time monitoring | 23        |
| 4.4.3    | Probabilistic methods                   | 24        |
| 4.5      | Correlation between weather parameters  | 24        |
| 4.6      | Grey-box modelling                      | 24        |

|          |                                                                     |           |
|----------|---------------------------------------------------------------------|-----------|
| <b>5</b> | <b>METHODS</b>                                                      | <b>26</b> |
| 5.1      | Data analysis                                                       | 26        |
| 5.1.1    | The system                                                          | 26        |
| 5.1.2    | Sag-temperature relationship analysis                               | 27        |
| 5.1.3    | Modelling line temperature with a multiple linear regression model  | 28        |
| 5.1.4    | Calibrating the dynamic model of line temperature in Matlab         | 28        |
| 5.1.5    | Evaluation of dynamic line temperature model                        | 30        |
| 5.1.6    | Examination of the system behavior using the dynamic model          | 31        |
| 5.2      | Estimating a dynamic line temperature model for OL9                 | 31        |
| <b>6</b> | <b>RESULTS</b>                                                      | <b>32</b> |
| 6.1      | Sag versus line temperature, ZL8                                    | 32        |
| 6.2      | Result from multiple regression                                     | 34        |
| 6.3      | Calibration results for dynamic line temperature model              | 35        |
| 6.4      | The influence of weather parameters on conductor temperature change | 40        |
| 6.5      | Time constants and step responses                                   | 41        |
| 6.6      | Worst-case simulation                                               | 44        |
| 6.7      | Possible rating of the two lines                                    | 46        |
| <b>7</b> | <b>DISCUSSION</b>                                                   | <b>48</b> |
| 7.1      | Analysis of ambient conditions and line temperature                 | 48        |
| 7.2      | The usefulness of the line temperature model                        | 48        |
| 7.3      | Possible weaknesses of the dynamic line temperature model           | 48        |
| 7.4      | Implications from results of possible ratings                       | 48        |
| 7.5      | The simplified wind model term                                      | 49        |
| 7.6      | Time constants and times for reaching temperature limit             | 49        |
| 7.7      | Variations along the line                                           | 50        |
| 7.8      | Sag-line temperature correlation                                    | 50        |
| 7.9      | Suggestion of uprating method                                       | 51        |
| <b>8</b> | <b>REFERENCES</b>                                                   | <b>53</b> |

# Appendices

Number of Pages

|                                                                        |    |
|------------------------------------------------------------------------|----|
| <b>APPENDIX</b>                                                        | pp |
| 1 - Measured line temperature plotted versus other measured parameters | 5  |
| 2 – Profile images of measured spans                                   | 2  |

# 1 Introduction

As the demand for energy increases, as well as demand for renewable energy, Vattenfall, as network owner, receives many requests to connect new wind power to the grid. Since the wind power has to be located at places where the wind is adequately strong the system has to adjust to the location of the wind farm rather than the other way around. This means that in order to connect the wind farms to the grid new overhead lines must sometimes be built or old ones reinforced. The building of new lines is a very costly and time-consuming process as it can take years for applications to go through the regulation system. Public opinion of new overhead lines can also slow down the process. Reinforcing old lines is also very expensive as the lines must be taken out of service for an extensive time. Therefore it is of big interest for Vattenfall to examine if the capacity of the lines is underrated.

Overhead line ratings (maximum current capacity) for these lines are based on the maximum allowable temperature of the conductor. The maximum allowable temperature is a temperature that is set so that the conductors will not at any condition during their lifetime get closer to the ground than the minimum electrical clearance distance, which is set by regulations. The minimum clearance distance is set to ensure public safety. A person getting too close to a high voltage electrical conductor could result in a flashover that could lead deadly currents through the passing person. This is why the safety aspect of overhead lines is so important and why an uprating of lines should be done carefully, backed up by both measurements and theory.

The sag of the line increases when the line elongates due to increasing temperature, mechanic load and time. The temperature of the conductor is dependent on conductor properties, line current and ambient conditions.

Today's line ratings are based solely on worst case assumptions of weather conditions. This means that the full capacity of the line is not used. This master thesis project is one part of a research project at Vattenfall which intends to uprate overhead lines for wind power insertion to the grid. If one can find a correlation between wind speed at nacelle (the generator house of the wind turbine) height and wind speed at line height wind power could be installed and connected to the grid to utilize a larger part of the actual capacity, since high wind gives high load on the line at the same time as high wind cools the line efficiently. The wind power could also be cut off to lower the load on the line in emergency cases when wind speed at line height would not cool the line enough as a means to ensure the line safety.

## **1.1 Purpose of the master thesis project**

The purpose of this master thesis was to investigate the relationships between the parameters that affect the line temperature and sag of overhead lines using measured data and literature search and to increase the knowledge in general about the sag and line temperature behavior at Vattenfall.

Specific aims were to:

- Identify correlations between the measured parameters.
- Highlight differences between the two overhead lines.
- Find existing calculation procedures and methods in literature.
- Give recommendations concerning the load capacity as a function of all involved parameters.

## **1.2 About the report**

This master thesis report will first go through some general theory about the Swedish grid (to put the measurements into context), about overhead lines in general and ACSR (*Aluminum Conductor Steel Reinforced*) conductors. The procedure at the operation center regarding the use of today's ratings will be shortly described. The measurement chapter deals with the data collecting measurement system. The theory chapter is the outcome of the literature search and gives equations for sag behavior and line temperature change behavior as well as a brief introduction to grey-box modelling. Methods of uprating are also described in this chapter. The methods chapter describes the procedure of estimating models for line temperature and sag. The report finishes with results from model estimation and simulations and discussion of results as well as some suggestions of future work.

## 2 Background

### 2.1 The Swedish grid

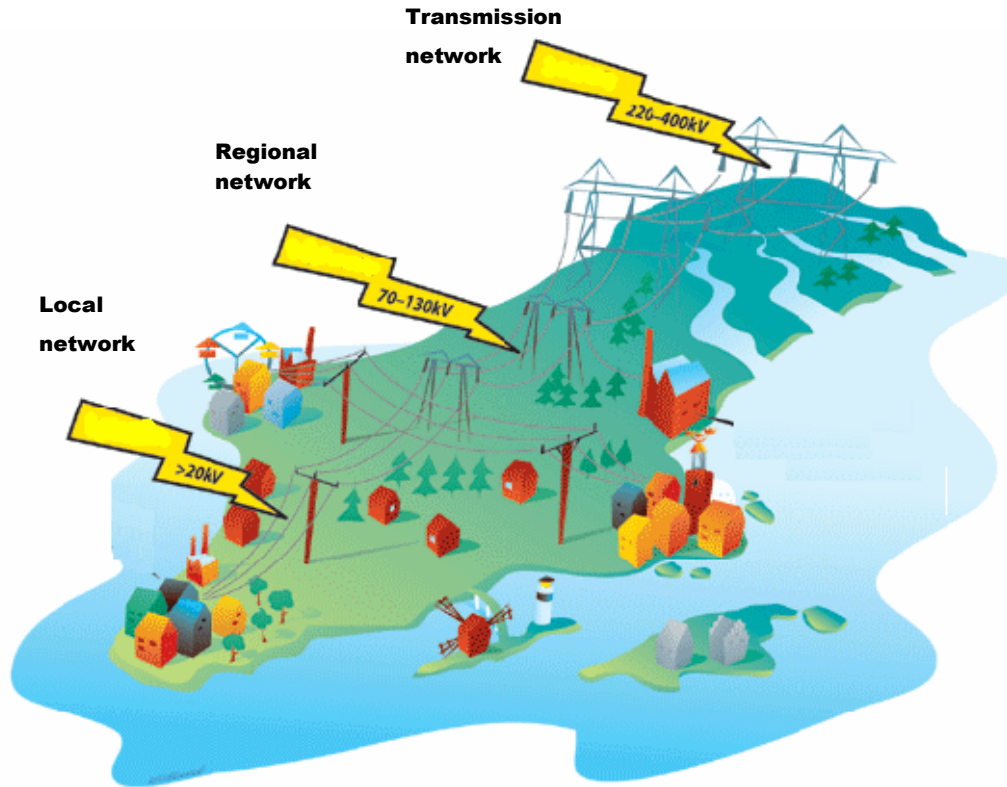


**Figure 2.1: Voltage levels of the Swedish electrical grid, (modified from [12])**

The Swedish electrical grid is divided into different voltage levels (Figure 2.1) [12]. The transmission network has the highest voltage levels, at 400kV and 220kV, and is used for long-distance transportation of electricity. This part of the network is owned and operated by Svenska Kraftnät, owned by the Swedish state.

The electricity is transformed down to lower voltage levels in transformation stations and is then called the regional network. The regional networks are owned and operated by the bigger energy utility companies in Sweden of which Vattenfall is one. The voltage level for the regional network is 40kV to 130kV. The regional network transports electricity from the transmission network to the local networks or directly to large industrial electricity consumers.

The local network has voltage levels below 40kV. The local network distributes the electricity to the final consumers such as households. Local networks in Sweden are owned by several local operators.

## 2.2 Overhead lines

The most used method of electricity transport in transmission and sub-transmission systems is with overhead lines. The alternative to overhead lines is underground cables which are more expensive than overhead lines and therefore not as common.



**Figure 2.2: Overhead lines with different structures, [8] and [4].**

Overhead lines can be built with steel towers or wooden poles (Figure 2.2) and can have different conductor materials. Higher voltage levels on the line require bigger and stronger structures. The conductors are held up by the towers via insulator strings.

Overhead lines must always have a minimum electrical clearance due to public safety. The safety distance for 130 kV overhead lines in Sweden is 7,4 m above ground for an area with detailed planning and 6,4 m for areas without detailed planning [19].

## 2.3 ACSR conductors

There are several types of conductors that are used for overhead lines. The most common is the ACSR (*Aluminum Conductor Steel Reinforced*) conductors [3]. Other types of conductors are all aluminum, copper and aluminum alloy. The desirable properties of a conductor are that it has low resistivity and has sufficient strength to be able to carry its own weight and additional load for its entire lifetime. Copper has lower resistivity than aluminum, which makes it a good electrical conductor, but has greater density, which means that the tower constructions and the insulators have to be heavier for copper conductors. This, together with the fact that aluminum is cheaper than copper, makes aluminum the more popular choice for overhead line design.

Aluminum is however a weaker material than copper and this is why the core of steel is added to the conductor, to increase its strength. [11]

The conductor is not solid but built up from aluminum and steel strands that are spiraled. One reason for stranding is the need for flexibility in the line. [11].

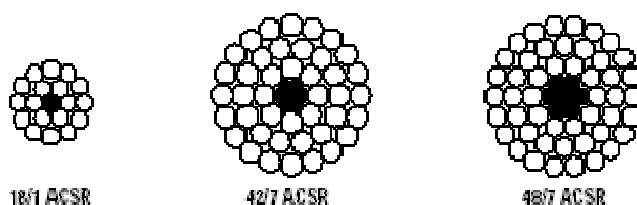


**Figure 2.3: Cross-sections of three types of ACSR conductors, [10]**

There are many different ACSR-conductors. The conductors that were measured on are of types 42/7 and 54/7. The first number stands for number of aluminum strands and the second for number of steel strands. In Figure 2.3 cross-sections of some ACSR conductors are shown.

The different build-up of aluminum and steel strands give the conductors different properties. The aluminum-to-steel area ratio affects the elastic modulus, the thermal elongation coefficient, the resistance of the conductor and the magnetic losses.

## **2.4 The monitoring at operation centers**

The work of everyday-monitoring of overhead line operation is done at the various operation centers. A visit at the operation center in Trollhättan gave this description of how the operation of monitoring overhead lines is currently run.

Today the current capacity of a line (the rating) is tabulated for different ambient temperatures and constant wind speed of 0.6 m/s for a maximum allowed line temperature of 50°C. A computer monitoring system that receives current data from the stations along the line uses two standard values for thermal rating, one for summer and one for winter. For 130kV lines the summer rating is based on an ambient temperature of 30°C and the winter rating on 10°C. If the monitoring system spots a current value in a station that is getting close to the rating an alarm goes off on the operators screen. The operator then decides what to do about the emergency. Overloads usually occur on cold winter days and then the operator knows from experience that the line can handle somewhat higher currents than the tabulated values.

## **3 Measurements**

### **3.1 Two measurement sites**

The measurement data used in this project comes from two 130kV overhead lines in southern Sweden, one in Brålanda and one in Björnåsen. The measurements began in July 2010, before the start of the master thesis project, and are still ongoing. The measured parameters are current, solar intensity, wind speed and direction, ambient temperature, relative humidity, conductor temperature and distance to ground.

The two measurement sites were selected on the basis of several important factors. The sites had to be located so that installation of equipment could go smoothly with easy access by car and also access to power to be able to supply heating of the measuring equipment. A good cellular network coverage was necessary for easy data transfer. High loading on the lines was preferred since the reason for measuring is trying to uprate the lines. If the loading already is so low that the full capacity is not used, then uprating would be unnecessary. An important factor on top of this was that the site had to have good shielding from wind to represent a hot spot on the line.

#### **3.1.1 Site OL9**

The line OL9 that runs through Brålanda was selected as previous simulations of the load flow had shown that this line possibly would reach limiting line loadings when connecting more wind power to the grid. A profile image of the chosen span for measurements is shown in Appendix 2. OL9 has a diameter of 27.8 mm and the span length at the site is 128 m.

#### **3.1.2 Site ZL8**

The line ZL8, which runs through Björnåsen, was chosen as the second line. It was chosen by means of its closeness to the coast, voltage level, dominating wind direction, the possibilities to perform planned interruptions, line loading and similarities and differences in line properties compared to OL9, such as diameter and span lengths. A profile image of the span is included in Appendix 2. The diameter of ZL8 is 39.2 mm and the span length is 247 m.

### **3.2 Measurement system**

The measurement systems that have been used are a Cordina box and a weather station. The measurement systems are identical for the two sites except for power supply system.



**Figure 3.1: The measurement system Cordinas installed on the line and the weather station on a pole beside the line**

The Cordinas box (Figure 3.1 and Figure 3.2) is a system which is installed on the line itself and measures line temperature, ambient temperature, current and distance to ground. The distance to ground is measured with a laser that reflects on the ground. The measurement system logs the data and communicates it to a computer at Vattenfall.



**Figure 3.2: The inside of the Cordina measurement system**

The weather station is located 6 meters beside the line (Figure 3.1 and Figure 3.3) and was placed at the height the Cordina box on the line at the time of installation. The wind measurement is done with a three-dimensional ultrasonic anemometer. The insolation sensor is placed so that no object will shadow it during times of high insolation. The ambient temperature and relative humidity sensors have radiation protection with ventilation that should limit the impact of solar radiation. The ambient temperature measurement from the weather station has in the master thesis project only been used in comparison to the ambient temperature measured with the Cordina box as to verify that the time tagging between the two systems has been correct. The relative humidity data has not been analysed.

The aspiration was to have data from two different lines to compare and also to have measurements from all seasons of the year. Unfortunately there were some technical difficulties with the Cordina measurements and communication system and therefore a lot of data is missing for July and August 2010 at Björnåsen. Complete data sets have not yet (May 2011) been obtained in Brålanda because the Cordina measurement has not been working and the line could not be taken out of service for repairs until late March 2011. The repairs still did not succeed in fixing the line temperature measurements which means that no line temperature data for Brålanda have yet been obtained.

After having shown unreasonable behaviour of “freezing” at one value the laser measurements in Björnåsen were improved with the placing of a white board on the ground under the box. This was done some time in October 2010.



**Figure 3.3: Close-up of the weather station**

### **3.3 Measurement data range**

The monthly max- and min-values for the measured parameter are displayed in Table 3.1. Measured data for periods not mentioned in Table 3.1 have also been collected but not taken into account within this thesis and are therefore not displayed in the table. High current was wanted as well as high line temperatures as the higher temperatures are of most interest within this project.

Notation for Table 3.1:

I – Current

V – Perpendicular wind speed

S – Insolation (Note that S also denotes span length in chapter 4.1)

$T_a$  – Ambient temperature

$T_c$  – Conductor temperature

**Table 3.1: Range for collected measurement data**

|                |           | I (A) |     | V (m/s) |     | S (W/ m <sup>2</sup> ) | T <sub>a</sub> (°C) |     | T <sub>c</sub> (°C) |     |
|----------------|-----------|-------|-----|---------|-----|------------------------|---------------------|-----|---------------------|-----|
|                |           | Min   | Max | Min     | Max | Max                    | Min                 | Max | Min                 | Max |
| Björnåsen, ZL8 | July      | 128   | 672 | 0.0     | 7.2 | 960                    | 11                  | 27  | 13                  | 42  |
|                | August    | 177   | 461 | 0.3     | 3.9 | 1012                   | 12                  | 20  | 13                  | 32  |
|                | September | 12    | 721 | 0.0     | 5.1 | 931                    | -1                  | 22  | -1                  | 34  |
|                | October   | 110   | 913 | 0.0     | 5.1 | 651                    | -7                  | 17  | -3                  | 40  |
|                | April     | 6     | 889 | 0.0     | 6.0 | 1034                   | -2                  | 22  | 0                   | 38  |
| Brålanda, OL9  | April     | 3     | 223 | 0.0     | 3.9 | 714                    | 1                   | 21  | -                   | -   |

## 4 Theory

### 4.1 Sag theory

The shape of a hanging line attached in its two ends can be described as a function of horizontal tension and weight per unit length [3].

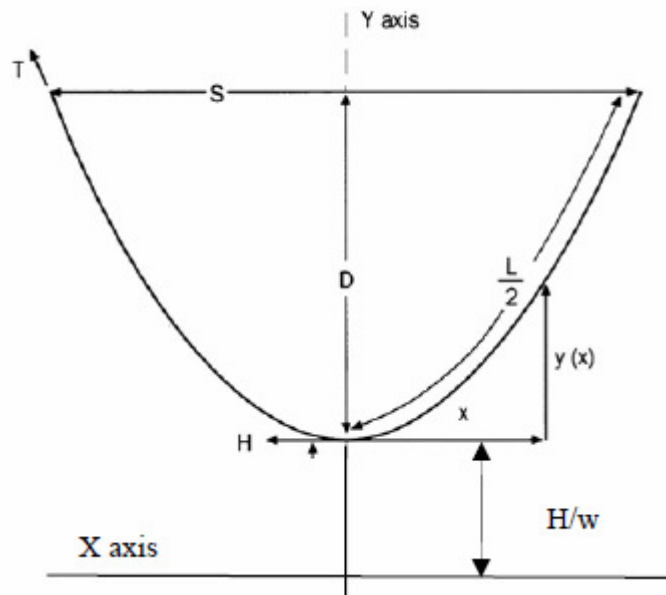


Figure 4.1: Illustration of conductor sag, [3]

Figure 4.1 illustrates the meaning of sag, span length and line length, where

$D$  = Sag (m)

$S$  = Span length (m)

$L$  = Line length (m)

$H$  = Horizontal component of tension (N)

$T$  = Total tension (N)

$w$  = weight per unit length of conductor. (N/m)

$x$  = horizontal distance from lowest point (m)

$y(x)$  = vertical distance from lowest point at  $x$  (m)

The shape of the hanging line can be described with an approximate parabolic equation or with a more exact hyperbolic catenary equation. The error due to parabolic approximation is very small except for very long, steep or deep spans. The parabolic equation, has the advantages that it easily shows the relationships between sag, tension, weight and span length [3].

The catenary equation is given by:

$$y(x) = \frac{H}{w} \cdot \left[ \cosh\left(\frac{w \cdot x}{H}\right) - 1 \right] \quad (4.1)$$

and the parabolic equation reads:

$$y(x) \cong \frac{w \cdot x^2}{2 \cdot H} \quad (4.2)$$

As the overhead lines are placed in the terrain the attachment points are not always placed on the same height. A span that has both attachment points at the same vertical level is called a level span. A span with its attachment points on different heights is called an inclined span. The calculation of sag for inclined spans is more complex than for level spans as the lowest point of the curve moves with changes in conductor length. Increasing length of the conductor moves the lowest point closer to the midpoint between the poles.

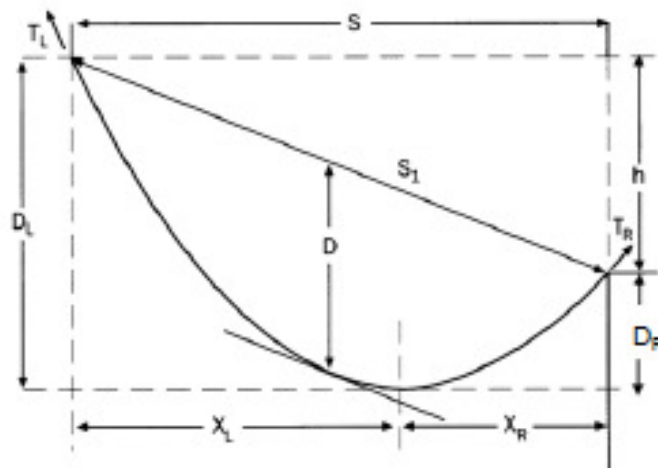


**Figure 4.2: Illustration of conductor sag for inclined span [3]**

The horizontal position of the lowest point for an inclined span can be described by:

$$x_r = \frac{S}{2} - \frac{H}{w} \sinh^{-1} \left[ \frac{h/2}{\frac{H}{w} \sinh \frac{S/2}{H/w}} \right] \quad (4.3)$$

where h is the difference in height between the two attachment points.

Figure 4.2 shows an inclined span. The sag for an inclined span will not describe the lowest point of the conductor but is defined in the middle of the span.

For a level span, using the parabolic approximation, the sag can be described by:

$$D = \frac{w \cdot S^2}{8 \cdot H} \quad (4.4)$$

It is apparent from (4.4) that sag is proportional to the square of the span length.

Sag can also be approximated as a function of line and span length as:

$$D = \sqrt{\frac{3 \cdot S \cdot (L - S)}{8}} \quad (4.5)$$

These equations assumes full flexibility of the conductor [3].

#### 4.1.1 Thermal elongation

The increase of sag with conductor temperature is due to expansion of the conductor material. The elongation can be described with a linear relationship [3]

$$\frac{\Delta L}{L} = \alpha_{AS} \cdot \Delta T_c \quad (4.6)$$

where  $\alpha_{AS}$  is the coefficient of linear thermal elongation.

The coefficient of linear thermal expansion is specific for each line as it depends on the aluminum-to-steel area ratio. Aluminum elongates with twice the rate as steel so the more aluminum the larger the coefficient of thermal expansion. These values are tabulated for different conductors [13].

When the conductor elongates due to temperature change the tension within the line also changes. In order to calculate the result accurately one needs to solve both equations for length and tension simultaneously [3].

Thermal elongation is described as an elastic elongation, which means that the process is reversible.

#### 4.1.2 Other line elongation causes

The conductor is also subject to other elongation causes than elastic thermal elongation such as long-time creep and mechanical ice and wind loads. High loads as well as creep causes plastic elongation (irreversible elongation) and changes the elastic modulus of the conductor.

When overhead lines are designed and installed they are installed so that the minimum clearance is to be ensured under all conditions that can apply under the lifetime of the conductor. The clearance must therefore hold for all the predictable ice and wind loads, for the maximum allowed conductor temperature and for the long-time creep (Figure 4.3).

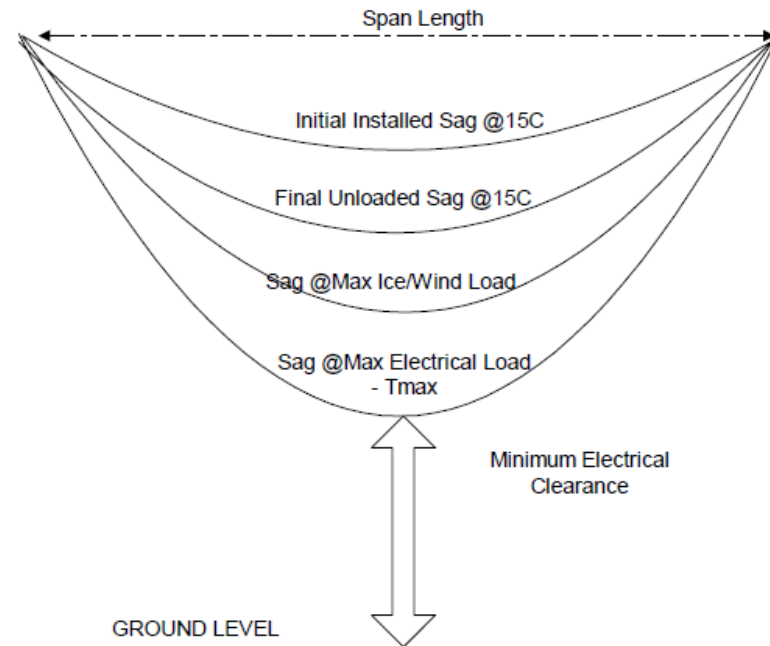


**Figure 4.3: Illustration of different causes to sag during a line's lifetime, [3]**

Values for final elastic modulus after wind and ice loading can be found in tables specified for each line type, see [13].

#### **4.1.3 Coupled spans**

The overhead line conductors are attached to the towers via insulator strings. Usually the insulator strings are somewhat free to move. The insulator moves when it is subjected to unequal forces at the bottom point, where the conductors are attached. The unequal forces arise when there is a difference in tension between spans. This means that any difference in tension between adjacent spans is equalized. [3] This also means that the sagging of one span is not isolated from the other spans and cannot accurately be calculated separately with the equations in the previous chapter.

#### 4.1.3.1 Ruling span method

Since the spans are coupled the sag can be approximated with the use of a so called ruling (or equivalent) span. A ruling span is a hypothetic span that captures the behaviour of the entire line section. The ruling span is defined as:

$$RS = \sqrt{\frac{S_1^3 + S_2^3 + \dots + S_n^3}{S_1 + S_2 + \dots + S_n}} \quad (4.7)$$

where

$RS$  – Ruling span for line section containing  $n$  spans

$S_1$  - Span length of first span

$S_n$  – Span length of  $n$  : th span

The sag in any one of the spans can then be calculated as

$$D_i = D_{RS} \left( \frac{S_i}{S_{RS}} \right)^2 \quad (4.8)$$

The ruling span method can be used for “reasonably” level spans, see [3].

#### 4.1.3.2 Numerical sag-tension calculations

A more accurate sag calculation of the sag can be done with numerical analysis. There are several computer programs that can do this. In this project a program called Sagsec was used. Sagsec lets one model the full line section and calculates, using finite element analysis, the forces on each insulator and the resulting sags of the line section can be determined.

## 4.2 Conductor temperature model

The model of heat gain in a conductor is derived from the general heat equation for a homogeneous and isotropic solid [2]:

$$\frac{\partial T}{\partial t} = \frac{\lambda}{\gamma c} \left( \frac{\partial^2 T}{\partial r^2} + \frac{1}{r} \frac{\partial T}{\partial r} + \frac{1}{r^2} \frac{\partial^2 T}{\partial \varphi^2} + \frac{\partial^2 T}{\partial z^2} \right) + \frac{q(T, \varphi, z, r, t)}{\gamma c} \quad (4.9)$$

$c$  = specific heat capacity (J/kgK)  
 $q$  = power per unit volume (W/m<sup>3</sup>)  
 $r$  = radius (m)  
 $T$  = temperature (K)  
 $t$  = time (s)  
 $z$  = axial length (m)  
 $\gamma$  = mass density (kg/m<sup>3</sup>)  
 $\lambda$  = thermal conductivity (W/mK)  
 $\varphi$  = azimuthal angle (rad)

This model can be simplified with the assumption that the conductor has cylindrical symmetry and semi-infinite length. This gives [2]:

$$\frac{\partial T}{\partial t} = \frac{\lambda}{\gamma c} \left( \frac{\partial^2 T}{\partial r^2} + \frac{1}{r} \frac{\partial T}{\partial r} \right) + \frac{q(T, \varphi, z, r, t)}{\gamma c} \quad (4.10)$$

If the radial temperature distribution is neglected then  $T_{av} = T_{core} = T_{surface}$ .

Mass per unit length,  $m$ , and power per unit length,  $P$ , is

$$\begin{aligned} m &= \gamma A \\ P &= qA \end{aligned} \quad (4.11)$$

where  $A$  is the cross-sectional area.

This reduces the conductor temperature model to a non-linear ordinary differential-equation on the form [2]:

$$mc \frac{dT}{dt} = P_j + P_s - P_r - P_w \quad (4.12)$$

where

$P_j$  = current heating  
 $P_s$  = solar heating  
 $P_r$  = radiative cooling  
 $P_w$  = wind cooling

[2] also includes the magnetic heating,  $P_M$ , in equation 4.12 but this term will be considered to be included in  $P_j$  within this master thesis project.

Mass per unit length and heat capacity will be considered constant within this report.

The conductor heat storage constant  $mc$  is calculated from [2]:

$$mc = m_a c_a + m_s c_s \quad (4.13)$$

where

$m_a$  = mass per unit length for aluminum section (kg/m)

$m_s$  = mass per unit length for steel section (kg/m)

$c_a$  = specific heat capacity for aluminum (J/kgK)

$c_s$  = specific heat capacity for steel (J/kgK)

The values of mass and heat capacity are taken from tabulated values [2],

The cooling and heating terms of the model will now be described individually.

#### 4.2.1 Current heating

The size of current heating depends on the size of the load current and the resistance at the prevailing conductor temperature. Magnetic heating and the heating due to skin effects also affects the size of current heating. [2]

The DC resistance of a conductor depends on the conductor area, the conductivity of aluminum, the lay lengths (the axial length of a whole turn in the spiral for the strands) and temperature. [6].

The AC resistance is higher than the DC resistance due to the so called skin effects. Skin effect refers to the tendency of the alternating current to flow near the surface of the conductor, this reducing the effective area and hence increasing the resistance. The skin effect increases with increasing frequency [11], decreases with increasing current density and increases with conductor diameter [6].

The number of layers of aluminum in the conductor affects the current heating characteristics. The strands are spiraled in opposite directions for every layer to avoid unwinding of the wire. This means that odd layer conductors behave differently than conductors with an even number of layers. [6]

An approximate method for calculating the current heating for steel cored conductors is [2].

$$P_j = k_j R_{AC} \cdot (1 + \alpha \cdot (T - 20)) \cdot I_{AC}^2 \quad (4.14)$$

where

$k_j$  = estimated parameter

$R_{AC}$  = AC resistance at 20°C ( $\Omega$ )

$\alpha$  = temperature coefficient of resistance per degree ( $K^{-1}$ )

$I_{AC}$  = AC current (A)

In this project a tabulated value for the AC resistance at 20 degrees has been used and the value for the constant  $k_j$  been obtained through model estimation. This constant is thus assumed to take care of skin effects and conversion from DC to AC current and other effects. For a more complex current heating model, see [2].

#### 4.2.2 Solar heating

The conductor is heated from solar radiation. The amount of heat gain from solar radiation depends on the diameter of the conductor, its inclination to the horizontal plane, the absorptivity of the conductor, the direct solar radiation, the diffuse sky radiation and the reflected radiation. [2]

The measuring equipment for diffuse and direct solar radiation is however expensive and needs regular attention which makes them difficult to use on remote sites. Measuring equipment for global solar radiation is cheap and reliable and is therefore more commonly used in these types of projects, including this. This means that the model is simplified to only depend on absorptivity, the solar intensity and the conductor.

$$P_s = \alpha_s SD \quad (4.15)$$

where

$\alpha_s$  = absorptivity

S = solar radiation (W/m<sup>2</sup>)

D = conductor diameter (m)

The absorptivity is the fraction of the incoming solar radiation that is absorbed in the conductor. This value varies within the lifetime of the conductor. As the conductor gets older this value increases. There are different opinions in the literature about which values of absorptivity that should be used. [2] states that an absorptivity of 0.5 can be used for most purposes, together with an emissivity of 0.5 (see also following section 4.2.3).

#### 4.2.3 Radiative cooling

All bodies emit energy in the form of electromagnetic radiation [14]. The emissivity of a body is the fraction of the emitted energy and the energy a black body would have emitted at the same temperature. The emissivity depends on the material of the

surface, temperature, surface condition and wavelength distribution of the emitted energy. [1] The wavelength distribution for electrical conductors is mostly in the infrared spectrum. The emissivity of conductors increases with the age of the conductor. Empirical studies on ACSR conductors have shown that newly installed conductors can have an emissivity of 0.23 while old conductors can have an emissivity of 0.95. [1] The age dependence of the emissivity for ACSR conductors can be described by

$$\varepsilon = 0.23 + \frac{0.70 \cdot Y}{1.22 + Y} \quad (4.16)$$

where Y is the age of the conductor in years.

The relation is also shown in Figure 4.4.

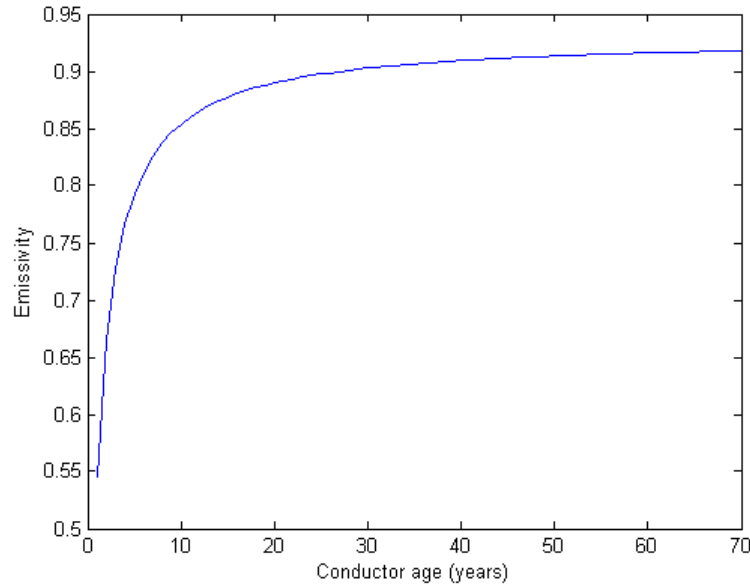


**Figure 4.4: Emissivity as a function of conductor age according to equation 4.16**

The total radiative cooling can be approximated with [9]

$$P_r = \frac{\pi}{2} D \sigma \left\{ \varepsilon_g [T_c^4 - T_g^4] + \varepsilon_d [T_c^4 - T_d^4] \right\} \quad (4.17)$$

where

$\sigma$  = Stefan - Boltzmann's constant

$\varepsilon_g$  = effective emissivity for conductor facing the ground

$\varepsilon_d$  = effective emissivity for conductor facing the sky

$T_c$  = temperature of the conductor in Kelvin

$T_g$  = temperature of the ground in Kelvin

$T_d$  = temperature of the sky in Kelvin

The emissivities are different for the top part of the conductor that faces the sky and the lower part that faces the ground. However, since the radiation loss is a small part of the total heat loss it is sufficiently accurate to use the overall ambient temperature,  $T_a$  [9].

$$P_r = \pi D \sigma \varepsilon \cdot (T_c^4 - T_a^4) \quad (4.18)$$

The emissivity and absorptivity of the conductor are closely related. Kirschoff's radiation law states that the monochromatic absorptivity ( $\alpha_s$ ) and emissivity ( $\varepsilon_s$ ) of a surface are equal,  $\alpha_s = \varepsilon_s$ . The incoming solar radiation lies mostly in the short wavelength spectrum and the radiation from the conductor mostly in the infrared. Therefore the infrared emissivity is used in (4.18). The short wavelength emissivity, and therefore the absorptivity according to above, can be approximated by: [1]

$$\begin{aligned} \alpha_s &= \varepsilon_s = \varepsilon + 0.2 \\ \alpha_s &= \varepsilon_s \leq 1 \end{aligned} \quad (4.19)$$

#### 4.2.4 Wind cooling

As the conductor due to current and solar heating usually is warmer than the surrounding air the conductor heats up the air adjacent to its surface. If there is a wind the heated air is carried away and new cold air can be heated by the conductor. Since heat leaves the conductor this has a cooling effect on it. If there is no wind there is still some measure of cooling since the density of the air heated by the conductor decreases and the warm air slowly rises. New air takes its place and this has a slow cooling effect on the conductor. In the case of no wind this is known as natural convective cooling and with wind is known as forced convective cooling.

In [7], three formulas are suggested for calculating wind cooling, one for no wind ( $q_{cn}$ ), one for low wind speed ( $q_{c1}$ ) and one for high wind speed ( $q_{c2}$ ). The air density, dynamic viscosity of air and thermal conductivity of air depend on the film temperature, which is the average between the conductor and the surrounding temperature, and values for these for different film temperatures are tabulated in [7] Of the three equations the one that gives the highest value at the present circumstances should always be used. The formulas in [7] are:

$$q_{c1} = \left[ 1.01 + 0.0372 \left( \frac{D \rho_f V_w}{\mu_f} \right)^{0.52} \right] k_f K_{angle} (T_c - T_a) \quad (4.20)$$

$$q_{c2} = 0.0119 \left( \frac{D \rho_f V_w}{\mu_f} \right)^{0.6} k_f K_{angle} (T_c - T_a)$$

(4.21)

$$q_{cn} = 0.0205 \rho_f^{0.5} D^{0.75} (T_c - T_a)^{1.25} \quad (4.22)$$

where

$\rho_f$  = air density

$\mu_f$  = dynamic viscosity of air

$k_f$  = thermal conductivity of air

$K_{angle}$  = wind direction factor (1 for perpendicular wind)

$V_w$  = wind speed

In [2] two formulas are suggested, one in the case of no wind and one for wind. These formulas are expressed using the dimensionless numbers Reynolds number, Grashof number, Nusselt number and Prandtl number.

For this project the modeling of convective cooling was simplified to

$$P_w = k_w \cdot (T_c - T_a) \cdot V^n \quad (4.23)$$

where

$k_w$  = estimated parameter

$V$  = perpendicular wind speed (m/s)

$n$  = estimated parameter

and the impact of natural convection was overlooked.

When measuring wind speed the standard is to measure ten-minute-mean values for the wind speed. This means that a lot of small changes in wind speed and wind angle are lost in the data. To avoid this loss of information a more accurate wind speed measurement equipment was installed that collects data every second, which is then used in the model as one-minute-mean values. The cooling effect from the wind is assumed to be only from the perpendicular wind so the data is first recalculated to a “cooling wind speed” which is the perpendicular resultant wind vector. This is the value of the wind speed that is used throughout this master thesis report.

The anemometer measures the wind speed and direction ten times per second and calculates a one-second-mean value for the vertical wind speed and the horizontal wind speed and direction. Figure 4.5 shows the coordinate system used to calculate the

cooling wind speed. Wind components in the X direction are parallel to the line and will not contribute to the cooling of the line.

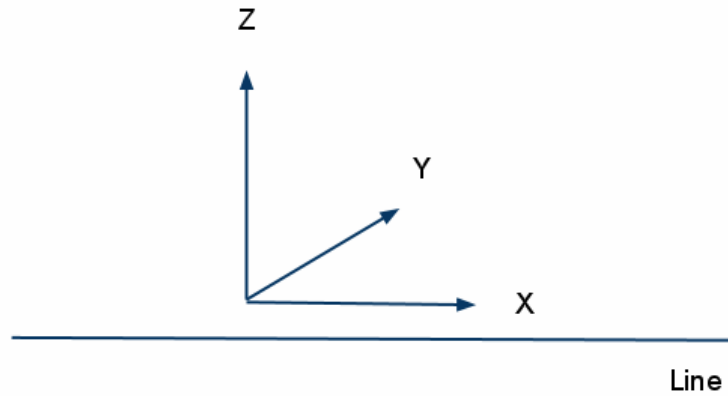


**Figure 4.5: Coordinate system for calculation of cooling wind speed. Only wind components in Y and Z direction will contribute to cooling.**

The horizontal wind speed vector is divided into perpendicular and parallel wind and a one-second-mean value for the cooling wind speed is calculated as:

$$V_{sec} = \sqrt{V_{Y,sec}^2 + V_{Z,sec}^2} \quad (4.24)$$

where

$V_{sec}$  - One - second - mean value of cooling wind speed

$V_{Y,sec}$  - One - second - mean value of wind components in Y - direction

$V_{Z,sec}$  - One - second - mean value of wind components in Z - direction

A one-minute-mean value of  $V_{sec}$  is the cooling wind speed  $V$  used in this thesis.

### 4.3 Thermal rating

Overhead lines that are thermally limited are designed and installed to have enough electrical clearance for all circumstances when the conductor temperature does not exceed its temperature limit. This temperature limit can be different for different lines. For these lines that are examined within this project the conductor temperature limit is 50°C.

The thermal rating of an overhead line is the calculated maximum allowed current. Thermal rating is calculated using:

$$I_{rating} = \sqrt{\frac{P_r(T_{max}) + P_w(T_{max}) - P_s}{R(T_{max})}} \quad (4.25)$$

This formula is derived from the conductor's steady-state heat balance.

#### 4.4 Line uprating

Line uprating is the process of making more capacity of a line available to use. Static rating is the traditional method of rating overhead lines. Static rating uses conservative assumptions about weather conditions. Common assumptions are wind speed of 0.6 m/s and full summer insolation. Assumptions about ambient temperature can vary and some utilities use seasonal static ratings with different ambient temperatures for different times of the year. At Vattenfall the ratings are based on an ambient temperature of 30°C in summer and 10°C in the winter for 130kV lines.

As the electricity market was deregulated the uprating of overhead lines has become more popular. There are several ways to uprate existing overhead lines. [5]. Some uprating methods include physical changes of the line, such as building higher towers, others are simpler, as the ones described below.

##### 4.4.1 Redefining weather conditions

The static ratings are usually much lower than the maximum possible rating. The easiest way of uprating is to just redefine the worst-case weather assumptions to less conservative by assuming a higher wind speed. This is however a risky method as field studies have shown that the wind is very low much more often than has been previously believed. [5]

##### 4.4.2 Dynamic Rating and real-time monitoring

Dynamic rating is a method that allows increased line load since it makes it possible to utilize the full capacity of the lines instead of being limited by a worst case scenario-approach. Dynamic rating requires measuring of several weather parameters at remote sites and a communication system that allows the data to be sent to the operations center. [5] The rating is calculated from actual weather conditions and is thus usually higher than the static ratings.

Real-time monitoring of sag, tension or conductor temperature is easier than dynamic rating based on real-time weather conditions. However, real-time monitoring demands more of the system operator. As where dynamic rating provides the operator with an allowed current load, simple real-time monitoring based rating requires the operator to estimate how large the load can be based on the properties of that specific line. [5]

Dynamic rating calculations can be based solely on real-time weather data or include calculations based on real-time conductor temperature, sag or tension data. If sag or tension are measured a correlation between them and conductor temperature can be calibrated.

#### **4.4.3 Probabilistic methods**

Weather data can be used to determine the probability that the maximum allowable temperature would be reached. A reasonably low risk could then be allowed and thus the rating could be increased. There are different ways to uprate lines in this way, with more or less complex ways. When doing this historical weather data can be collected from some nearby site. The methods can include the risk of an accident and the risk of an object or person being under the line. The methods can also include the load profile of the line and be combined with real-time monitoring. [5]

#### **4.5 Correlation between weather parameters**

The measured weather parameters within this project; solar intensity, ambient temperature and wind speed, are not entirely independent. If the solar intensity increases, the conductor temperature will increase, as well as the ambient temperature. The insolation that heats the ground and air causes instability in the atmospheric boundary layer which generates air movements (wind).

What this means in practice for the analysis is that it is often difficult to find periods where only one parameter is changing.

For figures describing correlations between measured weather parameters see Appendix 1.

#### **4.6 Grey-box modelling**

In empirical modelling of unknown systems one can take one of three different approaches, so called white-box, black-box or grey-box modelling. To search for a general physical model from known physical relationships is called white-box

modelling. To estimate a model based on measurement data without physical insight is black-box modelling. In between these two extremes is grey-box modelling which is searching for a model using the known physical parts of the system and using measurement data to estimate the unknown parts. Grey-box modelling will be used within this thesis for modelling of the line temperature. Grey-box modelling has the advantage that what is already known of the system is utilized and that the estimated parameters can have physical meaning. [18]

When building models it is natural to make approximations and simplifications. It is not meaningful to build a model that is more exact than is required from the purpose of the model. A simpler model with fewer variables gives shorter execution times for simulations in a computer.

For dynamic models the time constants of the modelled system describe how fast the system reacts to changes in the input variables. If the time constants in a system are very different the differential equations are called “stiff” and require particular numerical solvers.

When estimating the parameters in a dynamic model the main method is to minimize the prediction errors. The minimization method used within this thesis is the Output-Error method where the modelled output is compared to the measured value.

# 5 Methods

## 5.1 Data analysis

The analysis of the measurement data was at first approached as to find a completely unknown model of the system. This first approach was to make a multiple linear regression model of the line temperature. The second approach was to take the physical model found in literature and estimate the parameters to the measurement data (grey-box modelling).

The analysis of the data was done on data from line ZL8. For analysis of OL9, see section 5.2.

### 5.1.1 The system

The system that was to be examined is illustrated in Figure 5.1. This representation of the system shows that the parameters affecting line temperature are current, insolation, ambient temperature and wind speed. The line temperature in its turn affect the line sag. The dotted lines in the figure illustrates the correlations between insolation and ambient temperature and wind speed.

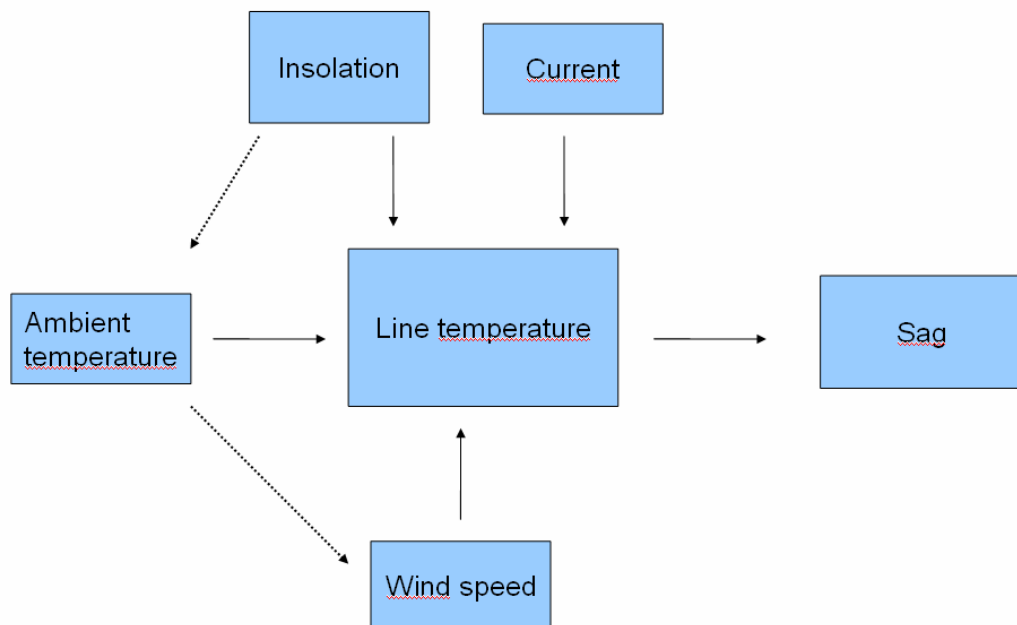


**Figure 5.1: Representation of the system describing internal relationships between system components according to regression model**

The system can also be described in functions of the cooling and heating as in Figure 5.2. In this figure the complexity of the system is visible where the only factor that

affects the line temperature independently of the line temperature itself is the solar heating. This figure describes the system according to the dynamic model.

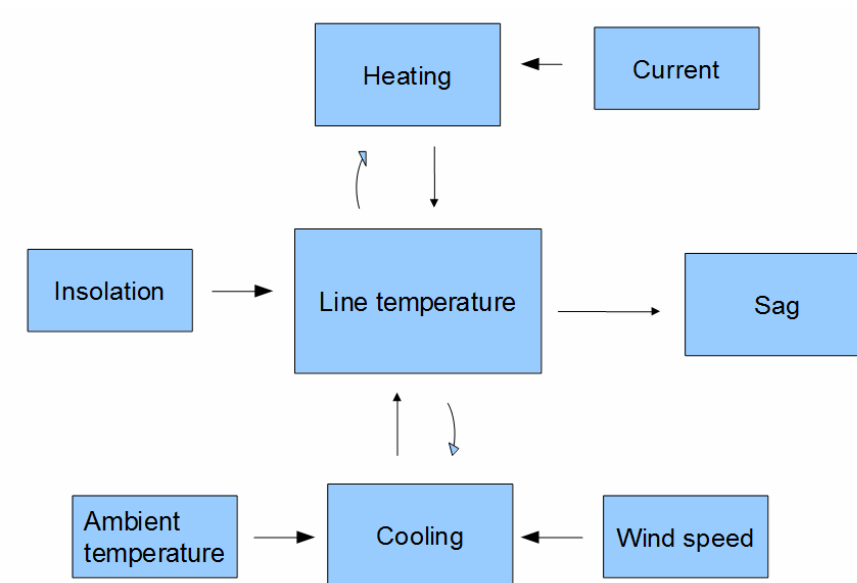


**Figure 5.2: Representation of the system describing internal relationships between system components according to dynamic model**

### 5.1.2 Sag-temperature relationship analysis

The sag-temperature relationship was analysed with three different approaches. The purpose was mainly to see whether the correlation was predictable and slow or if it would be non-linear and for example react faster at higher temperatures.

The correlation between measured distance to ground and measured line temperature was examined in plots for measurement periods July-October 2010 and April 2011. A simple linear regression curve was calculated with the Matlab function regress.

To see how much the 40 kg measurement system hanging on the line affected the behaviour and also to see how the coupled spans-effect affected measurements the line section was modelled with the computer program Sagsec with and without weight of measurement box and also for different temperatures. The measures of heights of attachment points and span lengths of the line section were taken from tables and from line-profiles. Since the total line section was long and finding properties of inclination had to be done by hand with a ruler on the profile images only the spans closest to the measurement span were modelled exactly and the rest of the section was approximated using the ruling span concept. The results for vertical position of the modelled weight

(representing the measurement box) were then plotted versus temperature change and compared to measurement data.

For calculations in Sagsec the values for tension and elasticity modulus used were the assumed final values for tension and elasticity modulus after maximum ice and wind load. The values used in the Sagsec-calculation were tension of 41.56MPa for 0°C, for an E-modulus of 60000MPa [13] and for an initial tension of 50MPa.

The approximate equation for sag as a function of span and line length (equation 4.5) was used with the linear thermal elongation model and the resulting sag-temperature relationship was compared to the Sagsec-calculated and the measurement-based relationship. The distance to ground measurements were translated into sag using proportions measured on the profile image of the span.

### **5.1.3 Modelling line temperature with a multiple linear regression model**

The first attempt of a line temperature model was to make a multiple linear regression of the line temperature dependence of ambient temperature, current, insolation and wind speed, based on the relations in Figure 5.1. The regression was performed with Matlab's function regress.

A problem that did arise when regression was performed in Matlab was the multicollinearity within the data. The high condition number of the data matrix indicates that the model is sensitive and not suitable to draw conclusions from about the physical behaviour of the model components. One of the objectives with the model was to be able to compare the magnitude of impact the different parameters had on the line temperature. The multicollinearity therefore makes the regression model not very useful, even though a good fit was achieved.

### **5.1.4 Calibrating the dynamic model of line temperature in Matlab**

As was found in literature [2], [7] the system is better described as in Figure 5.2 with dynamics. A grey-box model was therefore estimated using the structure of the non-linear ordinary differential equation described previously (section 4.2) The unknown parameters to be estimated were  $k_j$ ,  $k_w$ , and  $n$ . The Output-Error method was used for parameter estimation. This means that the output of the model, the line temperature, is compared to the measured line temperature in search for the best model fit.

The unknown parameters to be estimated are:

$$\theta = \begin{bmatrix} k_j \\ k_w \\ n \end{bmatrix} \quad (5.1)$$

The model error (prediction error) is defined as:

$$e(t, \theta) = y(t) - \hat{y}(t, \theta) \quad (5.2)$$

where

$y(t)$  – measured line temperature at time  $t$

$\hat{y}(t, \theta)$  – model output at time  $t$

The unknown parameters are found by the following minimization:

$$\begin{aligned} \hat{\theta} &= \arg \min_{\theta} V(\theta) \\ V(\theta) &= \sum e^2(t, \theta) \end{aligned} \quad (5.3)$$

where

$\hat{\theta}$  - the minimizing  $\theta$

$V$  – the loss function

Matlab includes several built-in ordinary differential equation solvers. For this purpose the solver ode15s was used, which uses a backward differentiation technique. The "s" in the name stands for "stiff" which means that the solver changes the step size depending on how fast the system is changing. A couple of other solvers were also examined on the model but seemed to be less accurate (ode45, ode23s). The possibility of using the simpler model as Euler forward was also examined but was slower and less accurate than the built-in solvers.

The ode-solvers in Matlab require continuous input data so the sampled measured data had to be interpolated before integration. The interpolation was done with the Matlab function `pchip`.

The optimization of the model was performed by using the Matlab function `fminsearch` which is a function that alters the specified coefficients and searches for a minimum of some function. The function that `fminsearch` should minimize was set to be the sum of square errors (equation 5.3). This means that in every iteration Matlab solves the differential equation for a new set of coefficients and compares this to the measured line temperature and decides if the square error is smaller than in the last iteration.

Parameter estimation using a calculated derivative from the equation to the measured line temperature derivative for every data point was also examined but failed as it was difficult to get a good estimation of the measured derivative.

The problem with optimization of non-linear functions is that there can be several local minima that cannot be separated from the global minima. This means that the result from optimization is not necessarily the best one.

Several attempts were made to estimate all the coefficients (including  $\alpha_s$  and  $\varepsilon$ ) but without result as the Matlab program froze after too many iterations. The optimization process therefore needed some manual testing of different combinations of coefficients and getting a feeling of which changes led to a better model. This led to an assumed higher absorptivity and emissivity, based on the age of the conductor (see section 4.2.3). The assumed emissivity for the 50-60 years old line was 0.91 and the corresponding absorptivity was estimated to be 0.99, since the absorptivity should be higher than the emissivity though not bigger than one. Optimization using the procedure described above could then be performed to find  $k_j$ ,  $k_w$  and  $n$ .

The model was calibrated on measurement data from a couple of days in September 2010 and validated on data from April 2011.

### **5.1.5 Evaluation of dynamic line temperature model**

Residuals were calculated and examined versus all the model parameters. For the model to be good there should be no patterns in the residuals, they should for example not be bigger for high currents than for low. This was used as a tool in the optimization process and was one of the reasons that the impact of insolation seemed to be underestimated at first with the low value of absorptivity.

### 5.1.6 Examination of the system behavior using the dynamic model

The dynamic model and the developed Matlab code were used to simulate different scenarios of interest. Step responses of current, wind speed and insolation were examined and time constants calculated from the results. The time constants were calculated as the number of minutes after the step change before the line temperature exceeds 63.2% of its final value. Extreme worst-case scenarios were modeled for the two lines. The contribution to the temperature change of the different heating and cooling terms was modeled using the coefficients derived in optimization of the dynamic model and the actual weather data and visually compared to the measured line temperature and the modeled line temperature. An estimation of the actual rating for a period was performed using actual weather data and the maximum allowed temperature assuming steady state for the rating.

## 5.2 Estimating a dynamic line temperature model for OL9

As the line temperature data for OL9 is missing a model could not be fitted for this line. In order to still try and get something out of the existing data and to be able to compare the two lines a model was estimated using the coefficients from the model for ZL8.

The two lines differ in diameter, steel-to-aluminum-ratio and resistance. These known differences were inserted in the model for OL9. The curve fitted coefficient in the current heating term,  $k_j$ , was assumed to be the same for OL9 as for ZL8. The solar heating and radiative cooling term for OL9 were assumed to have the same absorptivity and emissivity as ZL8. The simplified wind cooling term coefficient  $k_w$  for OL9 was assumed to be:

$$k_{w,OL9} = k_{w,ZL8} \frac{D_{OL9}^n}{D_{ZL8}^n} \quad (5.4)$$

with  $n = n_{ZL8}$ .

The line temperature that was modelled with these assumptions was then compared to the distance to ground measurement. Since the direct relation between distance to ground and line temperature not is known apart from a relative estimation no validation could however be done. The results from the OL9 data modelling must therefore be seen as very uncertain.

## 6 Results

### 6.1 Sag versus line temperature, ZL8

Figure 6.1 shows the measured values for distance to ground plotted versus the line temperature for measuring period July to October 2010. See appendix 2 for measures of the span.

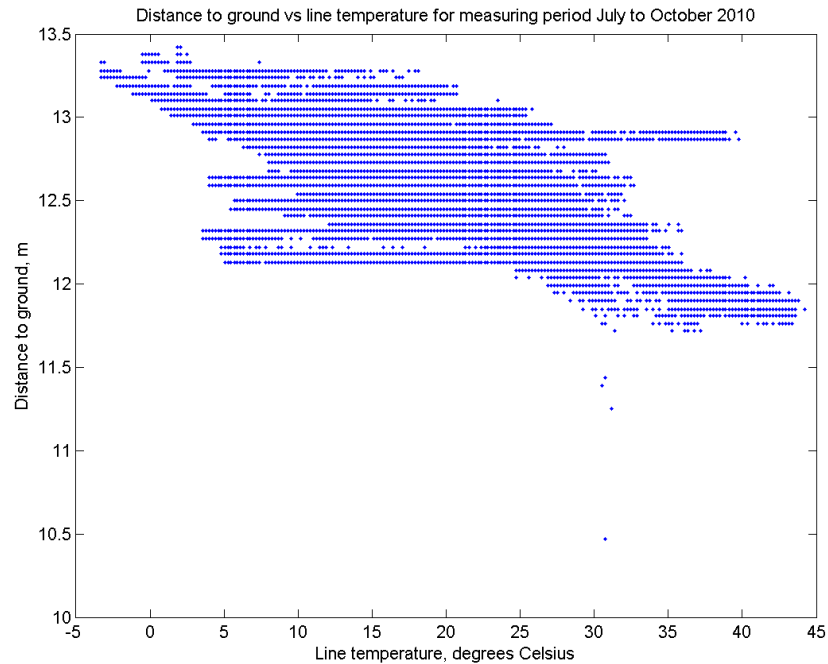


**Figure 6.1: Measured distance to ground versus line temperature for July to October 2010, ZL8**

The same relation for measuring period April 2011 is shown in Figure 6.2. The bigger spread of the data in Figure 6.1 can at least partly be explained by measurement difficulties. Figure 6.2 shows a linear relationship between distance to ground and line temperature for temperatures between 0°C and 35°C.

Linear regression performed on the April-data results gives equation 6.1.

$$Z = -0.037 \cdot T_c + 13,11 \quad (6.1)$$

where

Z = distance to ground (m)

$T_c$  = conductor temperature (°C),

with an  $R^2$ -value of 0,97.

This means that the model implies a decreasing distance to ground with 3,7 cm per degree Celsius.

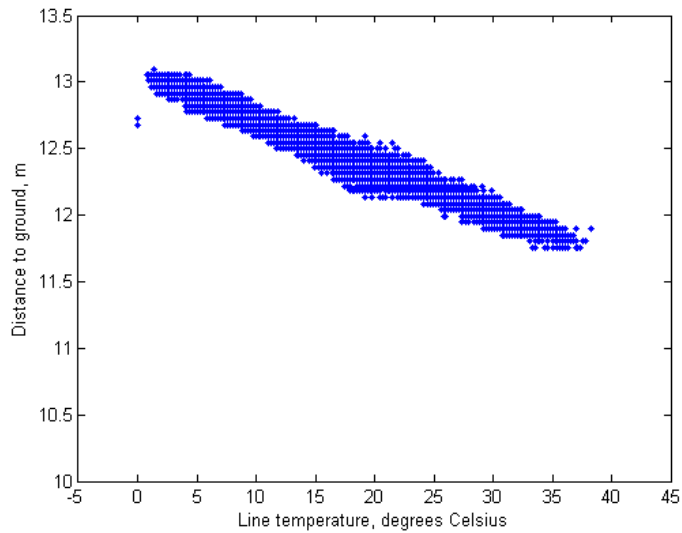


**Figure 6.2: Measured distance to ground versus line temperature for April 2011, ZL8**

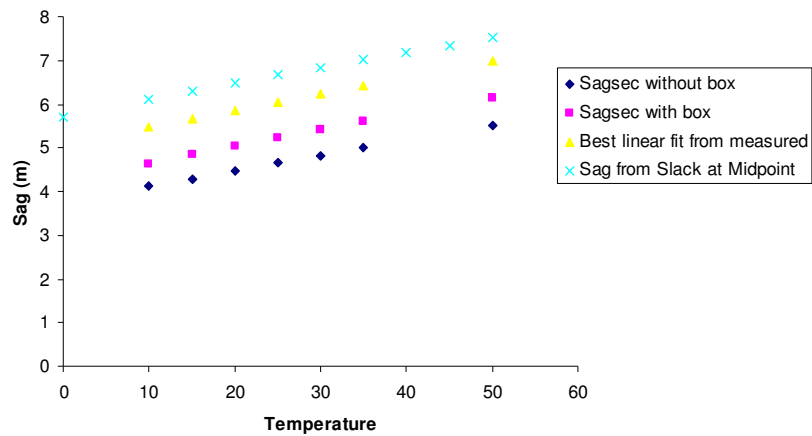


**Figure 6.3: Four curves describing sag versus line temperature, derived with different methods.**

The dark blue and the purple curves in Figure 6.3 shows the result of the Sagsec-calculation for different temperature with and without impact of the weight of the measurement box. The difference between the two curves indicates that the weight of

the box affects the measurements of ground distance with between 0,5-0,6 meters in comparison to how the result would have been without the impact of the weight. The both curves in Figure 6.3 show a linear relationship within the temperature range of 10 to 50°C.

Figure 6.3 also shows the result from sag-approximation for one isolated level-span using equation 4.5 plotted versus different conductor temperature changes, assuming a reference length of the conductor of 247,35 meters for 0 °C. Slack is the difference between line length and span length. All curves except the light blue describe the lowest point of the catenary. The light blue curve describes the midpoint of the span assuming a level span (see 4.1).

## 6.2 Result from multiple regression

Figure 6.4 shows the measured line temperature data and the regression model applied on the weather data for period beginning 10<sup>th</sup> of April 2011 and 5 days ahead. The calibration data period that was used was two days in September 2010. These results were not used further, see section 5.1.3.

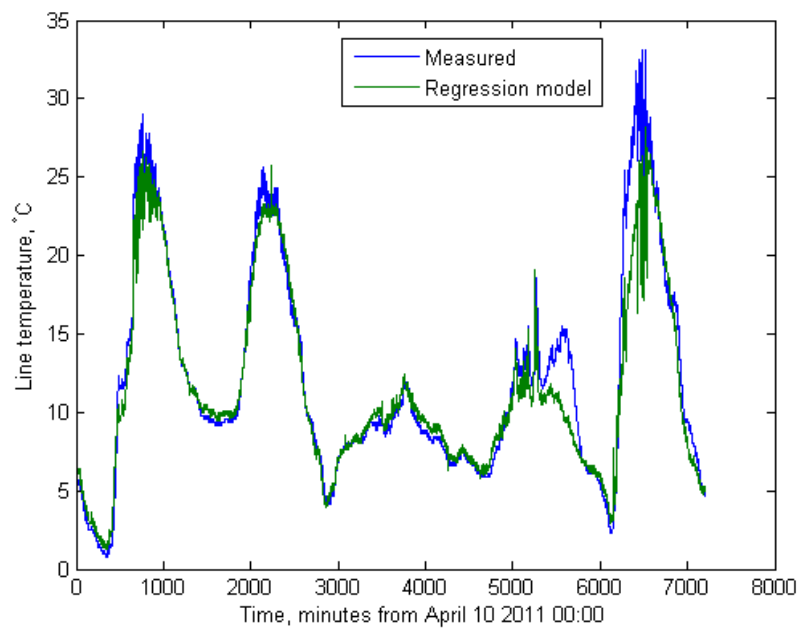


**Figure 6.4: Regression model and measured line temperature for validation data set**

The model from regression is

$$T_c = 7.96 \cdot 10^{-6} \cdot I^2 + 0.0106 \cdot S + 1.0041 \cdot T_a - 0.0223 \cdot V \quad (6.2)$$

where the line temperature  $T_c$  and ambient temperature  $T_a$  are measured in °C and  $V$  is perpendicular wind speed,  $I$  is current and  $S$  is insolation.

The condition number for the calibration data set is  $6.23 \cdot 10^5$ .

### 6.3 Calibration results for dynamic line temperature model

The final model was achieved with the values in Table 6.1. The estimated parameters are  $k_j$ ,  $n$  and  $k_w$  for ZL8.

**Table 6.1: Values used in dynamic model for ZL8 and OL9**

| Line                       | ZL8     | OL9     |
|----------------------------|---------|---------|
| D (mm)                     | 39,2    | 27,8    |
| Area (mm <sup>2</sup> )    | 910     | 454     |
| Area S (mm <sup>2</sup> )  | 44      | 52      |
| Area Al (mm <sup>2</sup> ) | 866     | 402     |
| alfa (K <sup>-1</sup> )    | 0.00403 | 0.00403 |
| R <sub>ac</sub> (Ω/km)     | 0.081   | 0.037   |
| k <sub>j</sub>             | 1.033   | 1.033   |
| α <sub>s</sub>             | 0.99    | 0.99    |
| ε                          | 0.91    | 0.91    |
| n                          | 0.5373  | 0.5373  |
| k <sub>w</sub>             | 2.066   | 1.7177  |

The result from validation on measurement period April 2011 of the dynamic model is shown in Figure 6.5. Modelling for shorter periods are shown in Figure 6.6 (April 11 to April 14) and in figure 6.7 (first of April).

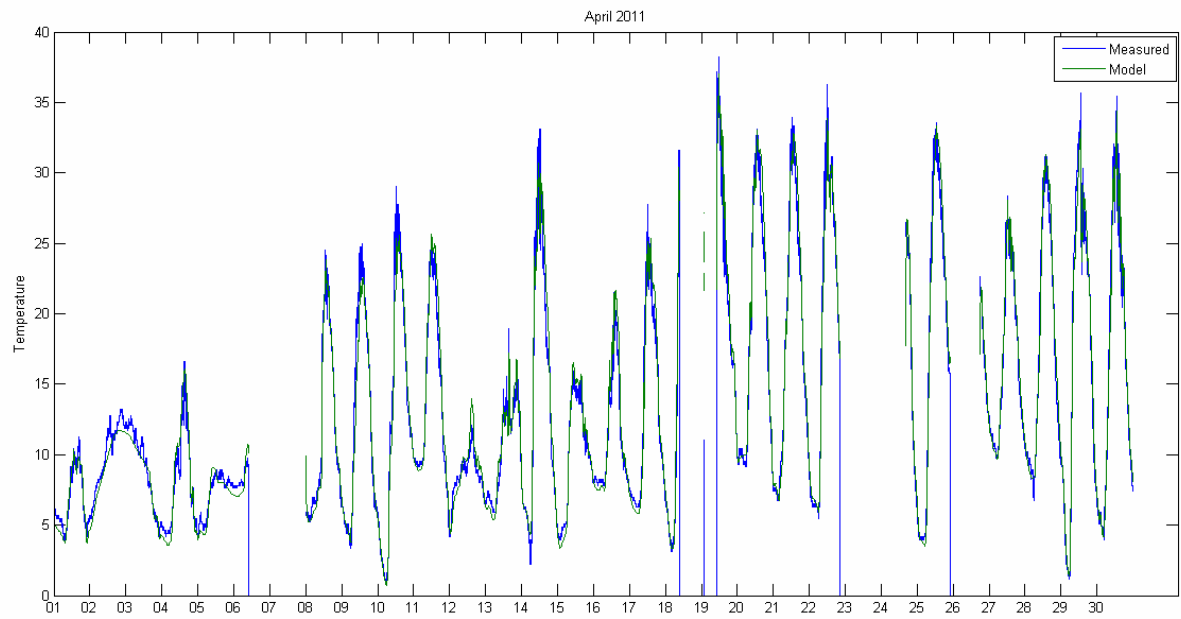


**Figure 6.5: Modelled and measured line temperature for validation data**

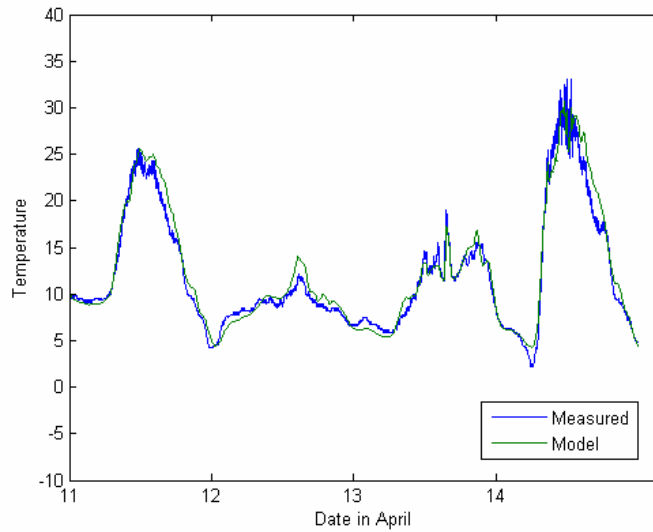


**Figure 6.6: Modelled and measured line temperature for four days in April**

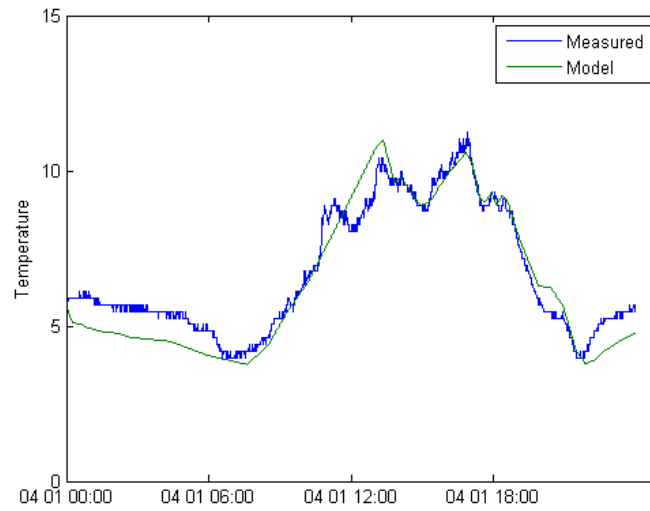


**Figure 6.7: Modelled and measured line temperature for one day in April**

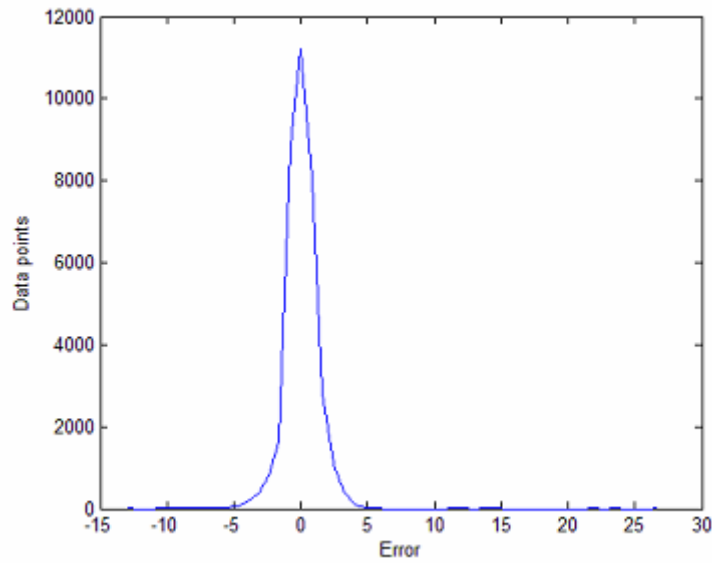


**Figure 6.8: Distribution of model error for the April data**

The model error distribution for the month of April is shown in Figure 6.8. Model error is defined in section 5.1.4 and is the difference between measured line temperature and model output.

The residuals of the model are plotted versus the measured parameters and displayed in Figure 6.9. In Figure 6.10 the residuals versus measured line temperature are plotted.

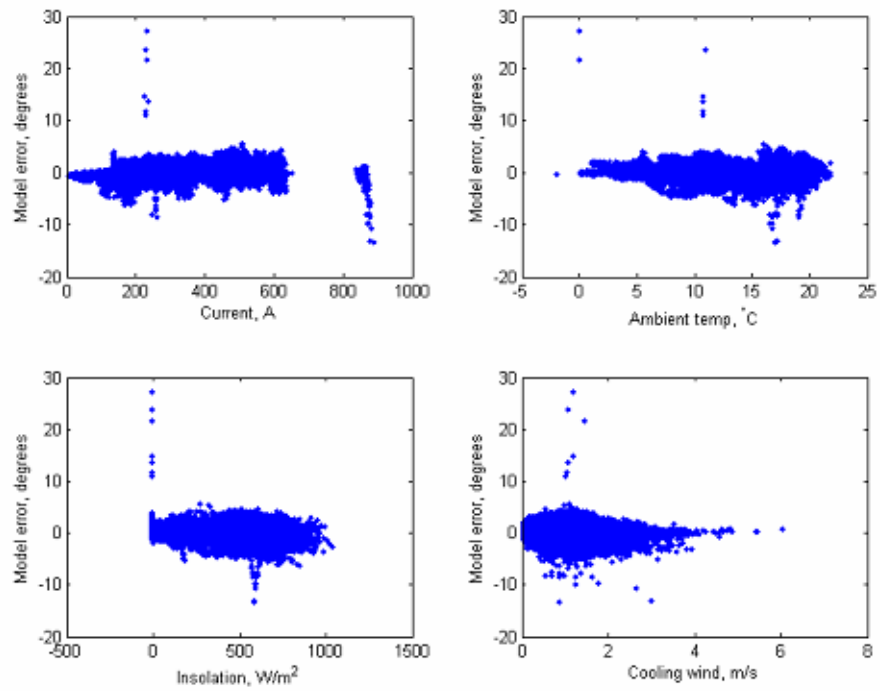


**Figure 6.9: Model error versus measured parameters for data July-October**

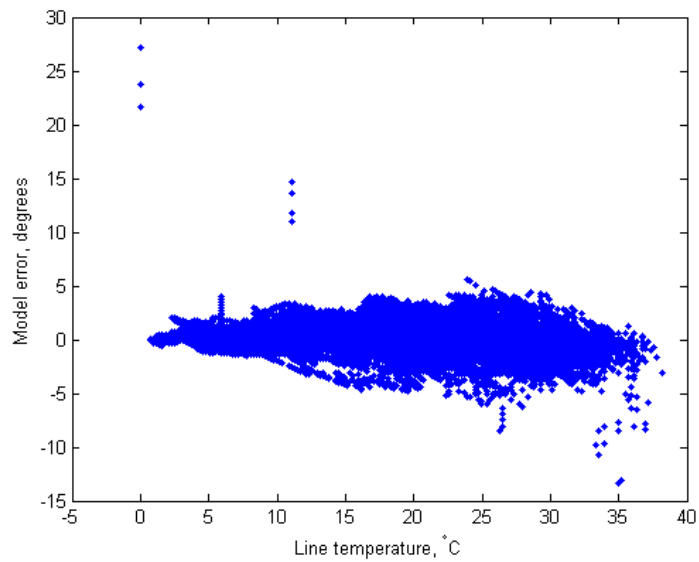


**Figure 6.10: Model error versus line temperature for data July-October**

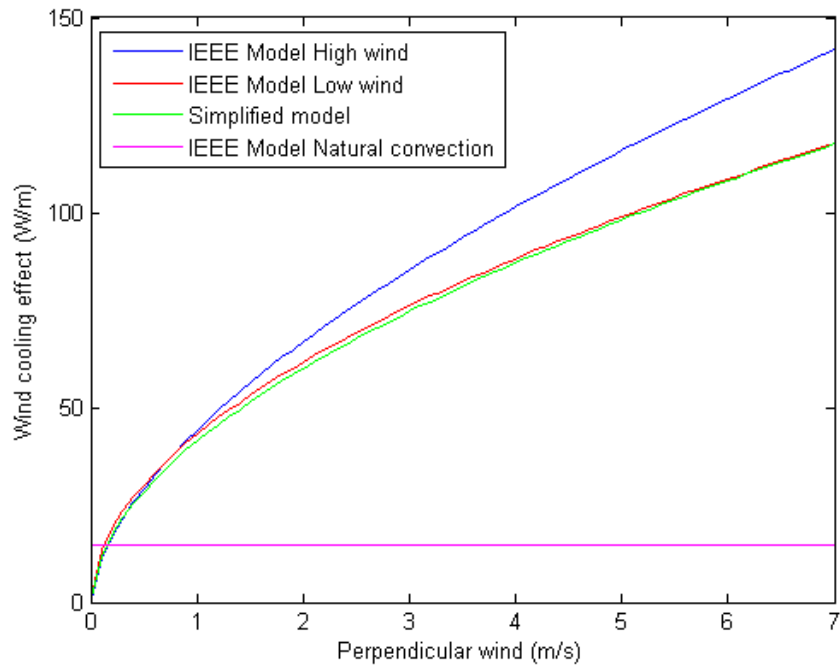


**Figure 6.11: Wind cooling effects versus perpendicular wind for model described in [7] and for simplified model (equation 4.23)**

The wind cooling term in the dynamic model is compared to the wind cooling terms suggested in [7] in Figure 6.11. The conditions used for the comparison is a conductor temperature of 45°C and an ambient temperature of 25°C. This gives a film temperature of 35°C and values for the dynamic viscosity of air, air density and thermal conductivity of air are taken from [7] using the values for an altitude of 0 meter.

The green line shows the simplified wind term model used in this project. The IEEE model suggests that the highest calculated wind cooling always should be used. That means that the IEEE model suggests using the purple curve up to about 0.2 m/s, then using the red curve until the blue curve crosses and then finally the blue curve.

#### 6.4 The influence of weather parameters on conductor temperature change

The sizes of the cooling and heating terms in the dynamic line temperature model are shown in Figure 6.12 for measuring period April 11 to April 16 2011. The curves represent the different terms, negative for cooling terms and positive for heating terms, and are calculated from the dynamic model coefficients and from actual weather data for these days. The actual measured line temperature has been used in the calculation and not the modelled line temperature.

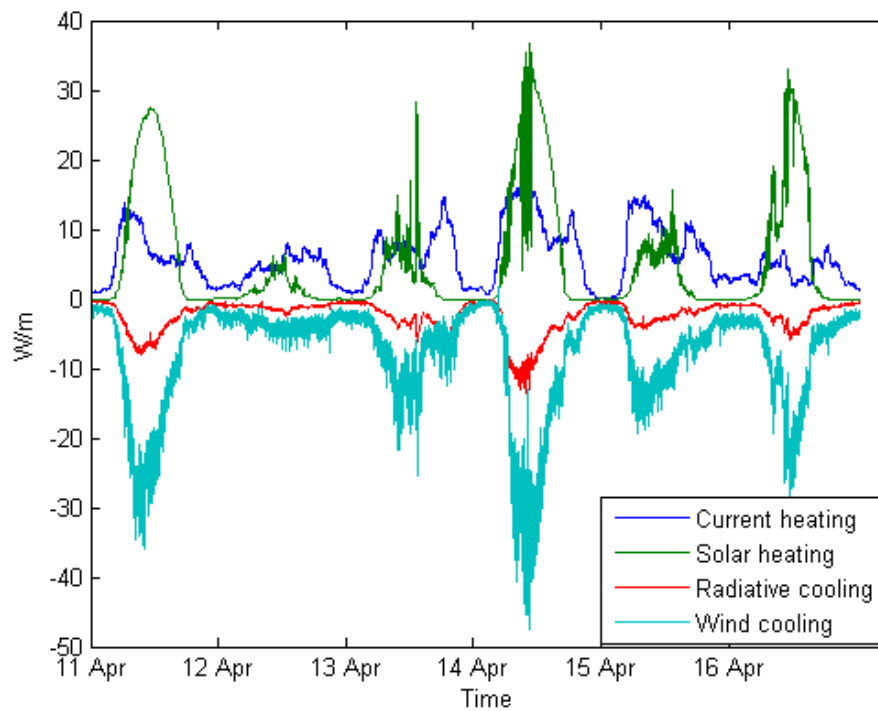


**Figure 6.12: The size of cooling and heating terms for six days in April**

The size of the wind term's variation with wind speed and line-ambient temperature difference is shown in Figure 6.13.

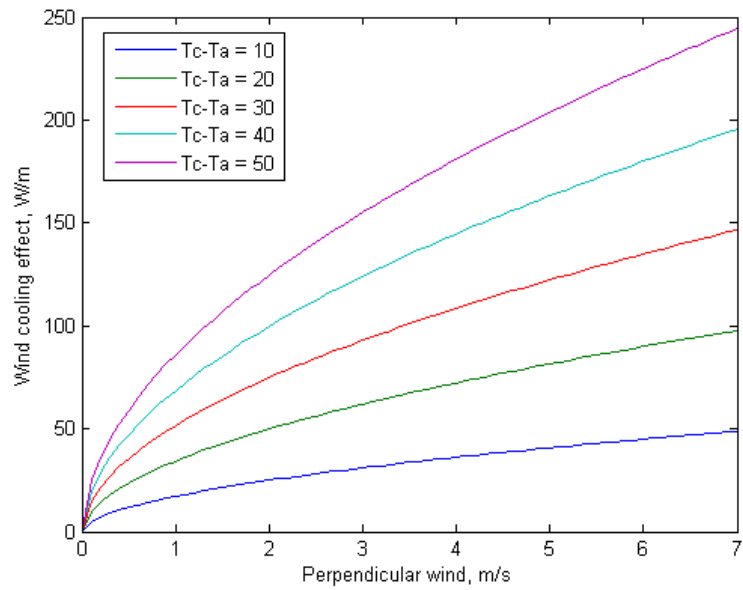


**Figure 6.13: Wind cooling effect versus wind speed for different temperature-differences**

## 6.5 Time constants and step responses

The line temperature step response for a current step from 200 to 800 amperes for different wind speeds between 0 to 5 m/s simulated with the dynamic model is shown in Figure 6.14. The time constants as well as the difference between end temperature and start temperature increase with decreasing wind speed.

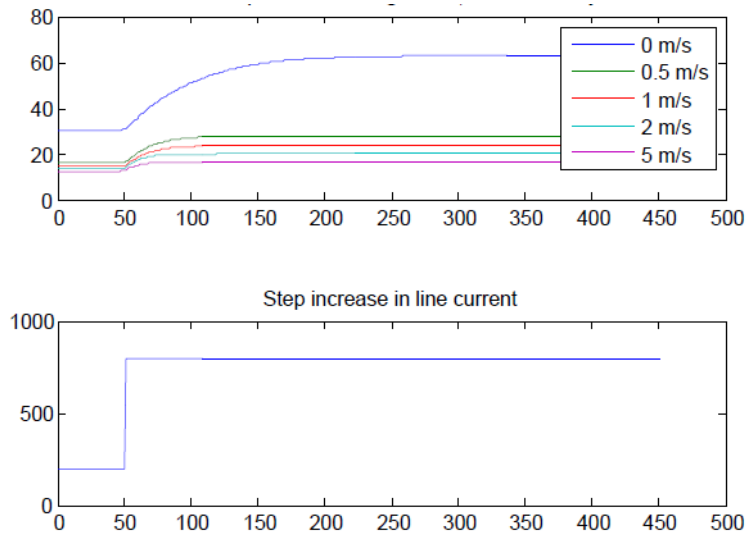


**Figure 6.14: Line temperature response to step change in current for different wind speeds (with ambient temperature 10°C, insolation 300W/m<sup>2</sup>)**

Step response simulation to a step increase in insolation from 0 to 1000 W/m<sup>2</sup> is shown in Figure 6.15. The three curves in the figure represent different constant current levels. The size of the temperature increase due to the insolation step is the same for all three current levels as well as the time constants.

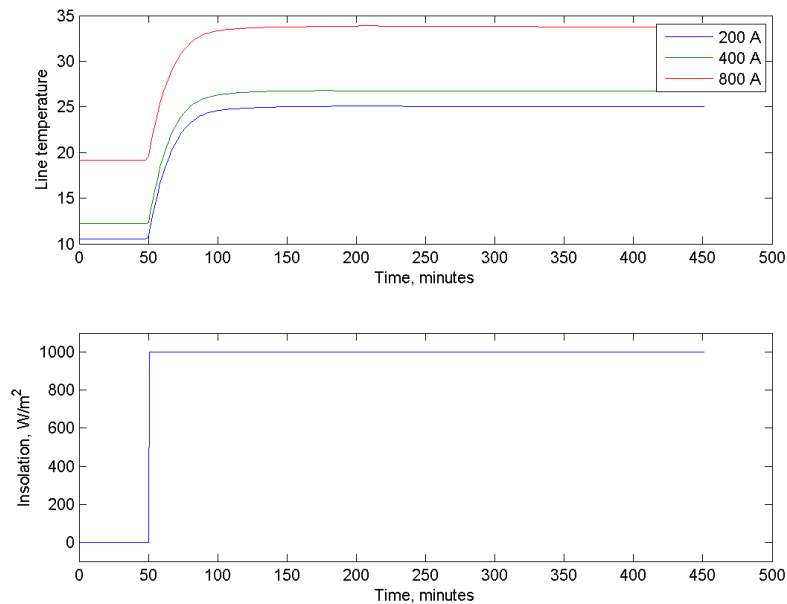


**Figure 6.15: Line temperature response to step change in insolation for different current levels (with ambient temperature 10°C, wind speed 1m/s)**

Line temperature step response to a step change in wind speed is shown in Figure 6.16. Two different step changes are simulated; one increasing wind speed from 0.2 to 5 m/s and one decreasing form 5 to 0.2 m/s. The temperature curves show that there is a difference between time constants for an increasing step and a decreasing step change.

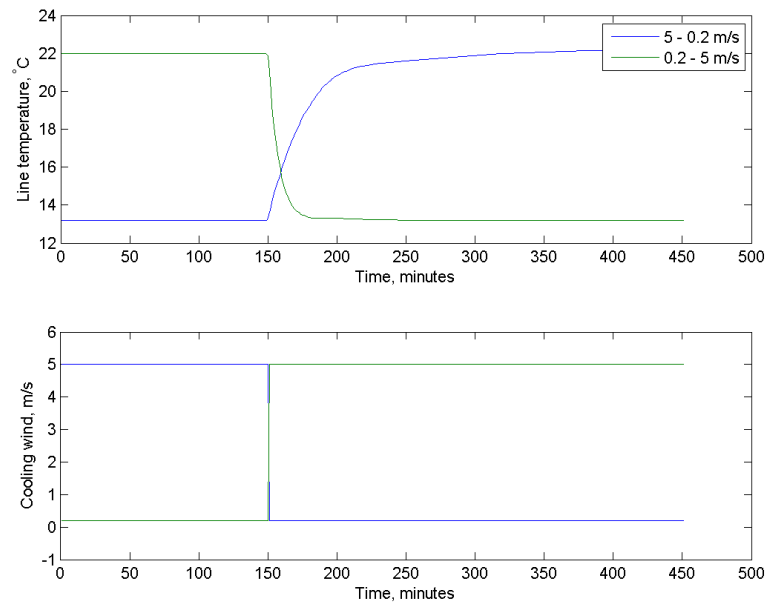


**Figure 6.16: Line temperature response to step changes in wind speed (ambient temperature 10°C, current 400A, insolation 300W/m<sup>2</sup>)**

The time constants and the step changes that are displayed in Figures 6.14 to 6.16 are also shown in Table 6.2. The table is colour-coded for emphasize on the variations and the results. The purple cells in the table describes the value that is different for the different curves, the green cells displays the resulting time constants and the blue cells display the resulting line temperature difference between final and initial value.

**Table 6.2: Step change simulations and results**

| Step in current | Wind (m/s) | Amb temp (°C) | Insolation (W/m <sup>2</sup> ) | Time constant (min) | Line temp start (°C) | Line temp stop (°C) | Temp-diff (°C) |
|-----------------|------------|---------------|--------------------------------|---------------------|----------------------|---------------------|----------------|
| 200-800 Ampere  | 0          | 10            | 300                            | 49                  | 31                   | 63                  | 32             |
|                 | 0,5        | 10            | 300                            | 19                  | 17                   | 28                  | 11             |
|                 | 1          | 10            | 300                            | 16                  | 15                   | 24                  | 9              |
|                 | 2          | 10            | 300                            | 10                  | 14                   | 20                  | 6              |
|                 | 5          | 10            | 300                            | 8                   | 12                   | 16                  | 4              |

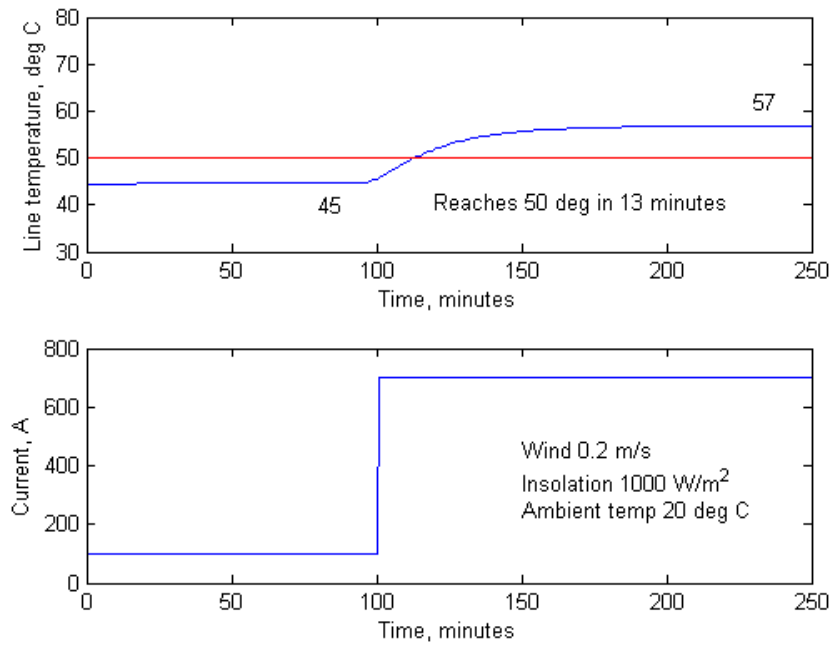
| Step in insolation      | Wind (m/s) | Amb temp (°C) | Insolation (W/m <sup>2</sup> ) | Time constant (min) | Line temp start (°C) | Line temp stop (°C) | Temp-diff (°C) |
|-------------------------|------------|---------------|--------------------------------|---------------------|----------------------|---------------------|----------------|
| 0-1000 W/m <sup>2</sup> | 1          | 10            | 200                            | 11                  | 10                   | 21                  | 11             |
|                         | 1          | 10            | 400                            | 11                  | 12                   | 22                  | 10             |
|                         | 1          | 10            | 800                            | 11                  | 11                   | 28                  | 11             |

| Step in wind speed | Current (A) | Amb temp (°C) | Insolation (W/m <sup>2</sup> ) | Time constant (min) | Line temp start (°C) | Line temp stop (°C) | Temp-diff (°C) |
|--------------------|-------------|---------------|--------------------------------|---------------------|----------------------|---------------------|----------------|
| 5-0.2 m/s          | 400         | 10            | 300                            | 24                  | 13                   | 22                  | 9              |
| 0.2-5 m/s          | 400         | 10            | 300                            | 6                   | 22                   | 13                  | -9             |

## 6.6 Worst-case simulation

Figures 6.17 and 6.18 show the differences in reaction time to a sudden current change for the ZL8 line and the OL9 line respectively. The ambient conditions are set to give a worst-case-scenario of constant wind speed at 0.2 m/s, constant insolation at 1000W/m<sup>2</sup> and constant ambient temperature of 20°C. The current step for ZL8 is from 100 amperes to 700 amperes. This gives an initial line temperature of 45 °C and a final line temperature of 57 °C. The temperature limit of 50 °C is also shown in the figure as the red line. The comparison between the two lines is made for different current steps that result in the same initial and final line temperature. The temperatures differ between the lines due to differences in resistance and diameter. The step change for the thinner line OL9 that gives the same temperatures as the previously mentioned step for line ZL8 is from 200 to 450 amperes. The temperature limit is reached in 13 minutes for ZL8 and in 8 minutes for OL9.



**Figure 6.17: Time to reach temperature limit for ZL8 with constant worst-case ambient conditions and sudden change in current**

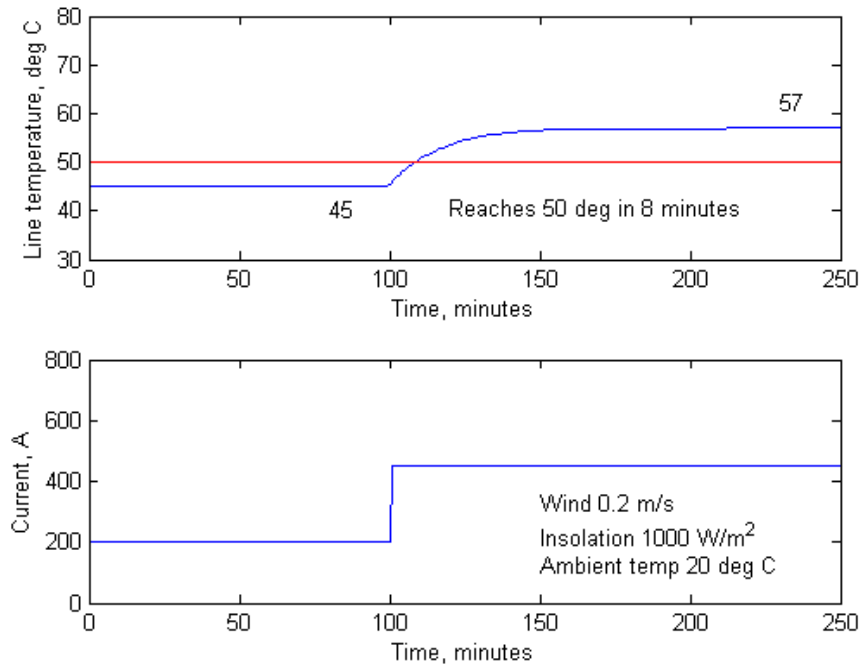


**Figure 6.18: Time to reach temperature limit for OL9 with constant worst-case ambient conditions and sudden change in current**

### 6.7 Possible rating of the two lines

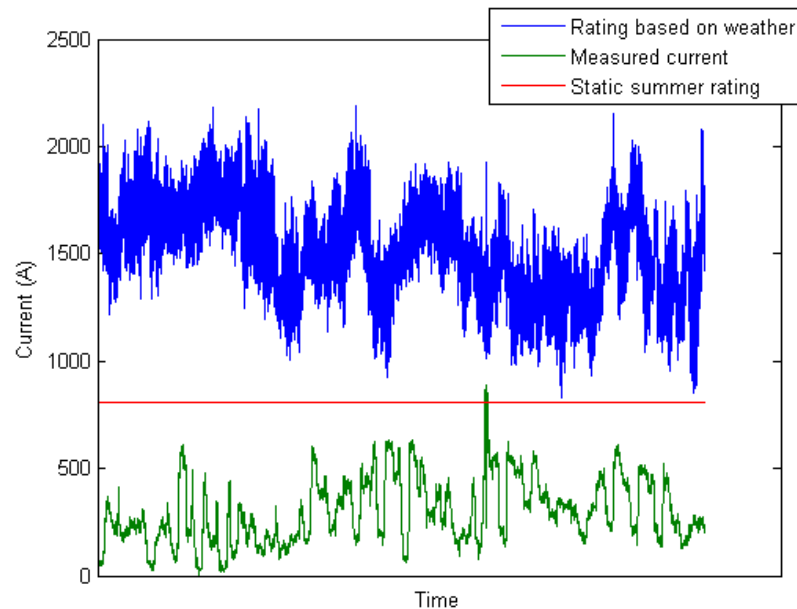


**Figure 6.19: Possible and static rating for ZL8 during April**

The possible rating calculated for every minute from equation 4.25 using measured weather data is displayed in Figure 6.19 for ZL8 and in Figure 6.20 for OL9 for available data in April 2011. The static summer rating for the two lines is the red line in the figures. The green line shows the measured current during that time.

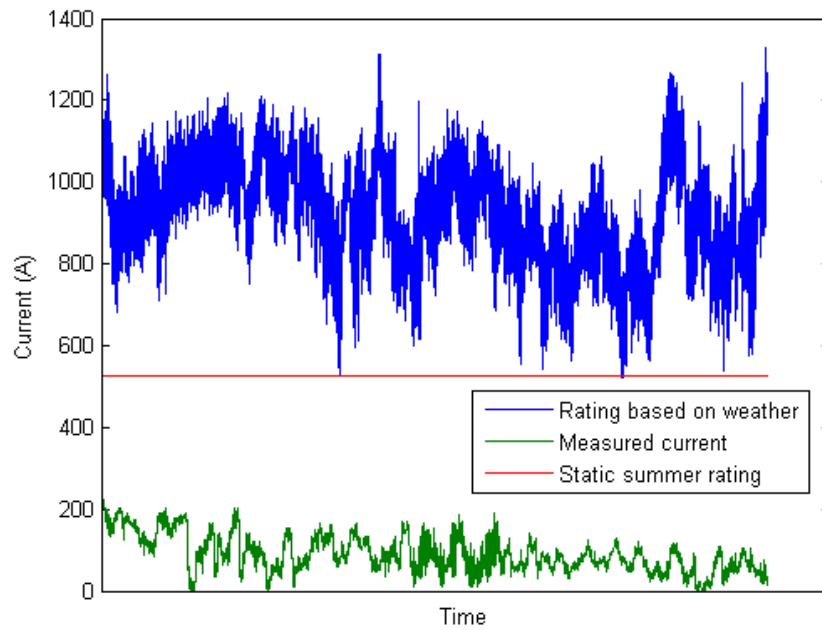


**Figure 6.20: Possible and static rating for OL9 during April**

## **7 Discussion**

### **7.1 Analysis of ambient conditions and line temperature**

A dynamic model has been estimated using the known physical properties of the system as described in literature and coefficients estimated for the two lines. Simulations using the dynamic model have been made to find time constants and line temperature behaviour at worst case and the contributions to heating and cooling from different weather parameters have been calculated based on the model.

The analysis within this thesis has not been to statistically look at all the available data and see how often certain scenarios happen but rather instead to find the behaviour and interactions between the input variables, illustrate and examine these behaviours and create and simulate interesting scenarios. There could thus be a lot of information remaining in the measurement data that could be analyzed in other ways.

### **7.2 The usefulness of the line temperature model**

The developed dynamic model can be used further to see under which circumstances the rating is the lowest and to simulate how often this would happen if new wind power were connected to the grid resulting in higher currents on the line.

### **7.3 Possible weaknesses of the dynamic line temperature model**

The dynamic model shows a good fit for the measured validation data set. The model error distribution shown in Figure 6.8 shows that for the validation data set the error was seldom bigger than 2.5 degrees. As seen in Figure 6.8 and also in Figure 6.9 there are some outliers with a big model error. The cause of these deviations has not been determined but a possible explanation is that the big errors occur at those times where bad data have been excluded from the data set and the model needed time to adjust.

The most interesting scenarios within this project are the line temperature behaviour at high currents and at resulting high temperatures and unfortunately there are not many data points that fulfil those criteria. This means that the model could have a worse fit for higher temperatures and/or higher currents than those within the validation data set.

### **7.4 Implications from results of possible ratings**

The possible rating shown in Figures 6.19 and 6.20 show that there was often a large margin between summer static rating and possible rating for April 2011. This supports

the belief that there is a lot to gain by changing the rating method for these lines. This analysis could be done for other periods as well for a fuller indication of the potential rating. The most interesting periods to examine would probably be the warmest and the coldest seasons.

Those few occasions when the possible rating gets close to the static rating should be further analysed when deciding on how to proceed with different rating methods at Vattenfall. If these occasions would show to appear due to low wind speed that also could be correlated with low wind speed at nacelle height the low rating would not be a problem for increased wind power connection.

The calculation of the possible rating is based on the assumptions of emissivity and absorptivity that was described in section 5.1.4. The emissivity of 0,91 coupled with a high absorptivity of 0,99 gives a more conservative line temperature than a low emissivity (0,5) that has been suggested (see section 4.2.2) for the measured line temperatures as the insolation contribution to the line temperature is bigger than the radiative cooling in everyday measured scenarios. However, when calculating the rating of the line the maximum line temperature (50°C for these lines) is used and this means that the radiative cooling term gets very big as soon as the ambient temperature is quite low and this effect gets bigger than the usually bigger insolation term that is not temperature dependent.

## **7.5 The simplified wind model term**

The simplified term for wind modelling compared to the complex wind terms as suggested in other literature (see section 4.2.4) shows to come close to the low wind term (Figure 6.11), for the examined temperature. This indicates that the simplified model wind term, when isolated from the model as whole, describes a more conservative wind cooling contribution than other models for higher wind speeds.

The figure also gives a sense of how much the natural convective cooling that is overlooked in the dynamic model would have contributed to cooling. The figure indicates that the theoretical natural convection would “guarantee” a perpendicular wind speed of 0.2 m/s at all times. This has however not been tested on the model or on the measurement data.

## **7.6 Time constants and times for reaching temperature limit**

The examination of time constants and step responses had two important purposes. One was to examine the impact of different line properties on the heat storing capacity and thus the reaction time. The other was to estimate how fast an operator has to be

able to cut down the wind power production when the line temperature suddenly rises due to sudden changes in order not to exceed the temperature limit.

The results from these simulations, as seen in Figures 6.17 and 6.18 implies that the operator would have about 10 minutes to react to a sudden increase in current at a worst-case ambient condition with a high initial temperature. For implementation the control center would thus have to have a scheme that allowed them to act within 10 minutes after a sudden increase in current.

The results also indicate that a thinner line would result in faster reactions to current changes. This would have to be considered if implementing any uprating method on the lines.

## **7.7 Variations along the line**

The measurements in this project have only been considering one point along each of the lines. The points were selected with one criteria that they would represent a “hot spot”, that is a point at the line likely to show the most extreme high line temperatures. Good wind shielding was therefore the criteria. An overhead line is usually not straight and the terrain can differ a lot along the line. As the wind direction is an important factor when deciding the magnitude of wind cooling it is likely that the situation can differ quite a lot between different parts of the line section. This should be considered in further analysis. There is also an ongoing debate within the field of dynamic rating whether line temperature measured in one point is suitable for real-time monitoring or if it is too local and tension and or sag should be measured instead. This matter will be discussed in a report from CIGRÉ coming fall 2011.

## **7.8 Sag-line temperature correlation**

Both methods for calculating the sag-temperature relationship, as well as measurement data, show that within the temperature range from 0 to 50°C the relationship is approximately linear. This is a good result for the project as it indicates that measuring the line temperature would be quite enough to roughly know the position of the line. It would not be necessary to know the exact position, as the design included buffers, but it is good that the sag does not suddenly increase faster with higher temperatures or acts in any other unpredictable way.

As for the agreement between measured distance to ground and theoretically calculated there is a good agreement between the rate with which the distance decreases with temperature but a worse agreement for the absolute distance to ground. As seen in Figure 6.3 the four curves have approximately the same slope but different intersection points. This could possibly be a result from uncertainty in the measures

manually done in the profile image (Appendix 2). When looking at the profile image one should be aware that the vertical scale is ten times bigger than the horizontal. As the horizontal position of the measurement system is not known, but assumed to be at the lowest point of the curve, and the ground under is very inclined a few meters error in the assumption of horizontal position could result in some vertical error.

## **7.9 Suggestion of uprating method**

The deregulation of the energy market around the world has been the driving force for line uprating. Prior to the deregulation the lines were designed with very generous clearance buffers and the conservative weather assumptions were widely accepted, but since then as the competition on the market gets tougher and the difficulties in transmission construction increases the energy utilities have come up with new solutions such as implementing real-time monitoring systems. [17]

An even newer trend is to combine the overhead line uprating with the increasing construction of wind power plants. Studies on this are made for example in Germany [16] and in England [15]. The wind power plants often need to be located where the existing network is designed for small loads [15]. Instead of reinforcements of the overhead lines the idea with this type of dynamic uprating is that strong wind gives high power production as well as adequate cooling of the overhead lines. As a safety measure the wind power production can also be turned off in case the temperature limit is reached.

For an implementation of an uprating method at Vattenfall with the purpose of inserting new wind power on old lines the results and experiences from this master thesis project would suggest a real-time monitoring system that measures the line temperature and has the possibility to cut down wind power production in emergency cases. This suggestion is based on a few findings. One is that it does not seem necessary to measure the sag of the line, as measurements as well as theoretical studies show that there is a predictable linear relationship between the line temperature and the sag. This is also supported by literature [5] that states that one can choose which one of line temperature, sag and tension that is to be measured for real-time monitoring as they can be translated to each other. However, information from the coming CIGRÉ report should also be considered, see section 7.7. Real-time monitoring is suggested rather than dynamic rating after the experience that measurement systems often can fail to deliver data and thus the fewer parameters that need to be measured, the better. This suggestion does however rely on the assumption that there is a clear correlation between low wind speed at line height at hot spots along the line and at nacelle height at the wind power locations so that emergency cut-downs of wind power production would be a very rare occasion. That means that further research must be done before any final conclusions on implementation.

Research will continue at Vattenfall with a pilot project for a real-time monitoring system beginning August 2011.

## 8 References

- [1] Black, W.Z., Rehberg, R.L., (1985). *Simplified model for steady state and real-time ampacity of overhead conductors*, IEEE transactions on power apparatus and systems, Vol. Pas-104, No. 10
- [2] CIGRÉ, (2002). *Thermal behaviour of overhead conductors*
- [3] CIGRÉ, (2007). *Sag-tension calculation methods for overhead lines*
- [4] Corren.se, (2011-05-24). [www.corren.se](http://www.corren.se)
- [5] EPRI, (2005). *Increased power flow guidebook*
- [6] IEEE, (1985). *AC Resistance of ACSR – Magnetic and temperature effects*, IEEE transactions on power apparatus and systems, Vol. PAS-104, No.6
- [7] IEEE, (2006). *IEEE Standard for calculating the current-temperature of bare overhead conductors*
- [8] Kungliga vetenskapsakademien, (2011-05-24). [www.kva.se](http://www.kva.se)
- [9] Morgan, V.T., (1982). *The thermal rating of overhead-line conductors Part I. The steady state thermal model*, Electric power systems research, 5 119-139
- [10] Pacific cabling solutions Ltd, (2011-05-24). [www.pacificcabling.com](http://www.pacificcabling.com)
- [11] Schavemaker, P., van der Sluis, L., (2009). *Electrical power system essentials*, John Wiley & Sons Ltd, England
- [12] Svensk energi, (2011-05-24). [www.svenskenergi.se/sv/Om-el/Elnatet/](http://www.svenskenergi.se/sv/Om-el/Elnatet/)
- [13] Svenska elektriska kommissionen, (1999). *Dimensionering av friledningar för starkström – Ledare*, Svensk standard SS 436 01 02
- [14] Young, H., Freedman, R., (2004). *University Physics*, 11<sup>th</sup> edition, Pearson Education, San Fransisco
- [15] Yip, T., Chang, A., Lloyd, G., Martin, A., Ferris, B., (2008). *Dynamic line rating protection for wind farm connections*, Developments in Power System azection, 693-697

[16] Ringelband, T. et al (2009). *Potential of improved wind integration by dynamic thermal rating of overhead lines*, PowerTech, 2009 IEEE Bucharest, 1-5

[17] CIGRÉ (2006). *Guide for selection of weather parameters for bare overhead conductor ratings*

[18] Glad, T., Ljung, L., (2004). *Modellbygge och simulering*, Studentlitteratur AB, Lund

[19] Elsäkerhetsverket, (2008). *ELSÄK-FS 2008:1, 7*

# Appendix 1

Measured line temperature plotted versus other measured parameters

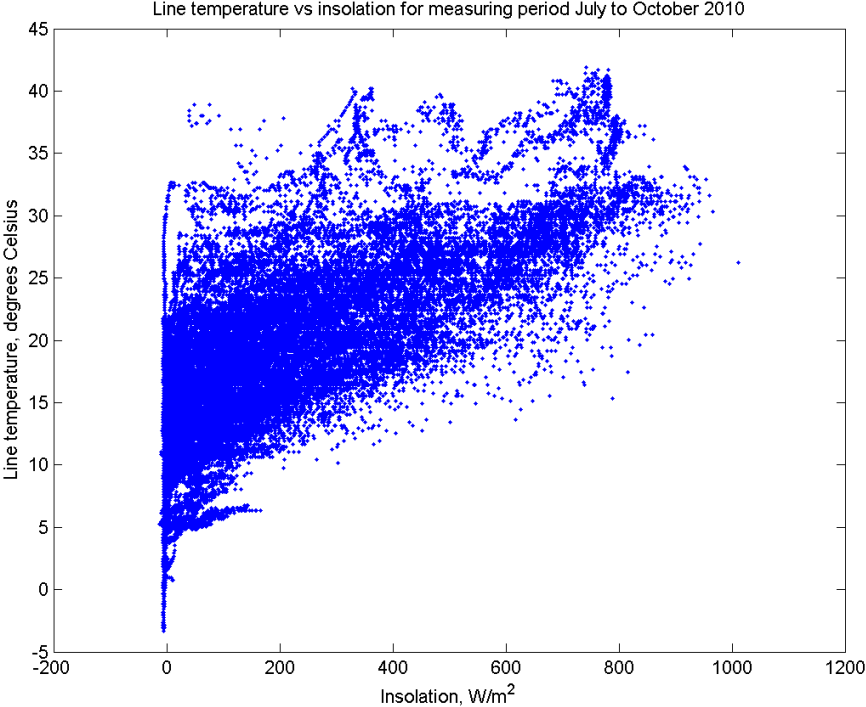
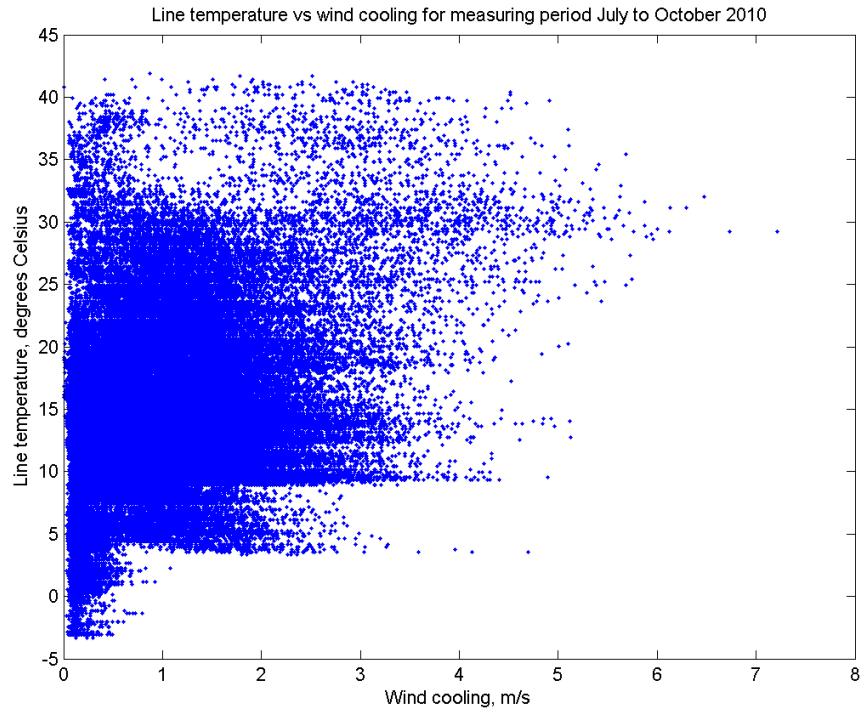
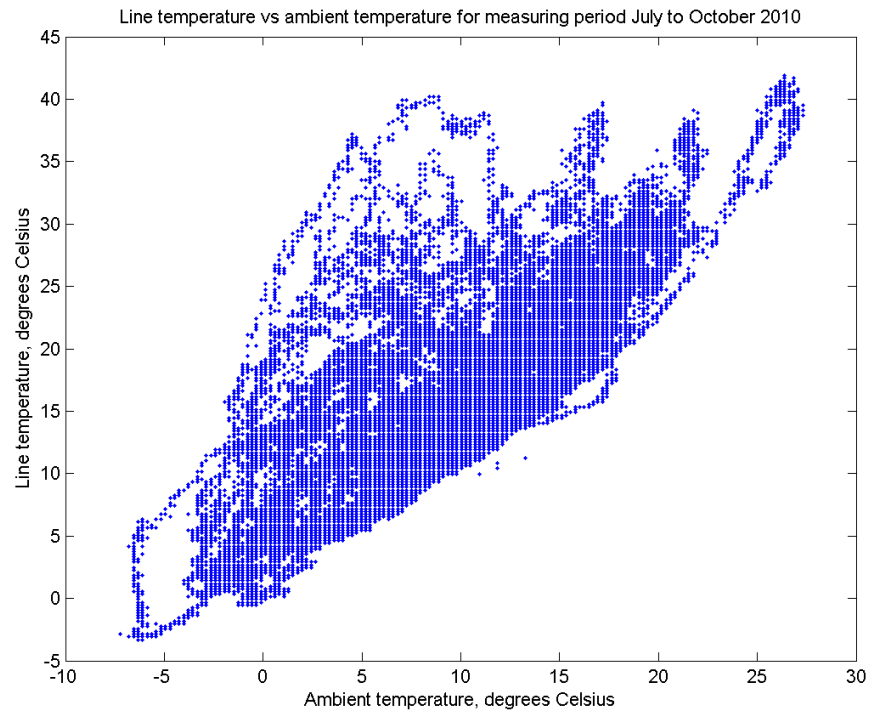


Figure A1.1: Measured line temperature versus measured insolation for period July 2010 to October 2010



**Figure A1.2: Measured line temperature versus measured perpendicular wind for period July 2010 to October 2010**



**Figure A1.3: Measured line temperature versus measured ambient temperature for period July 2010 to October 2010**

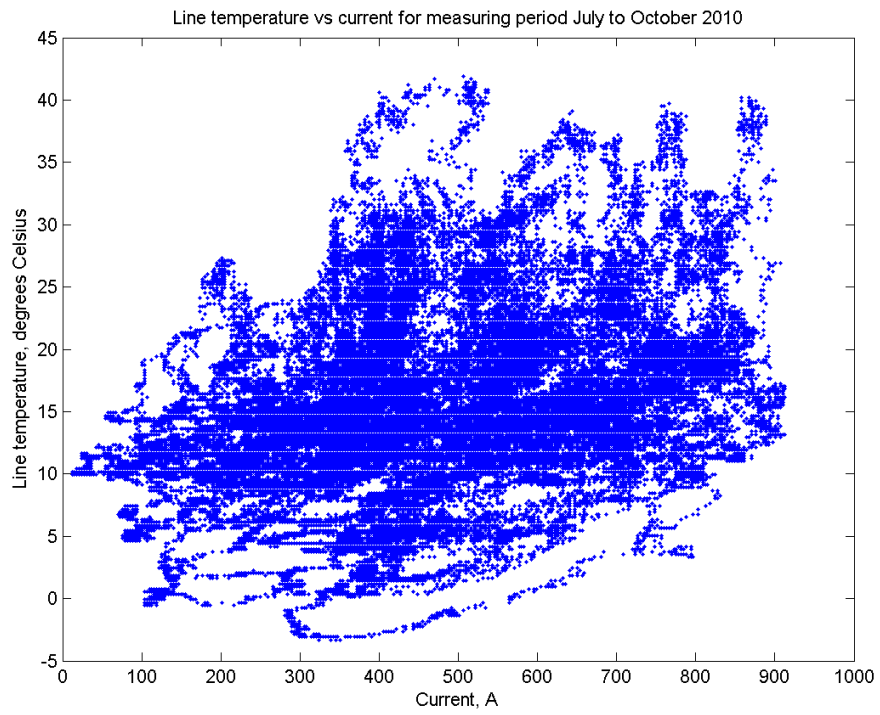


**Figure A1.4: Measured line temperature versus measured current for period July 2010 to October 2010**

## Correlations between measured ambient conditions

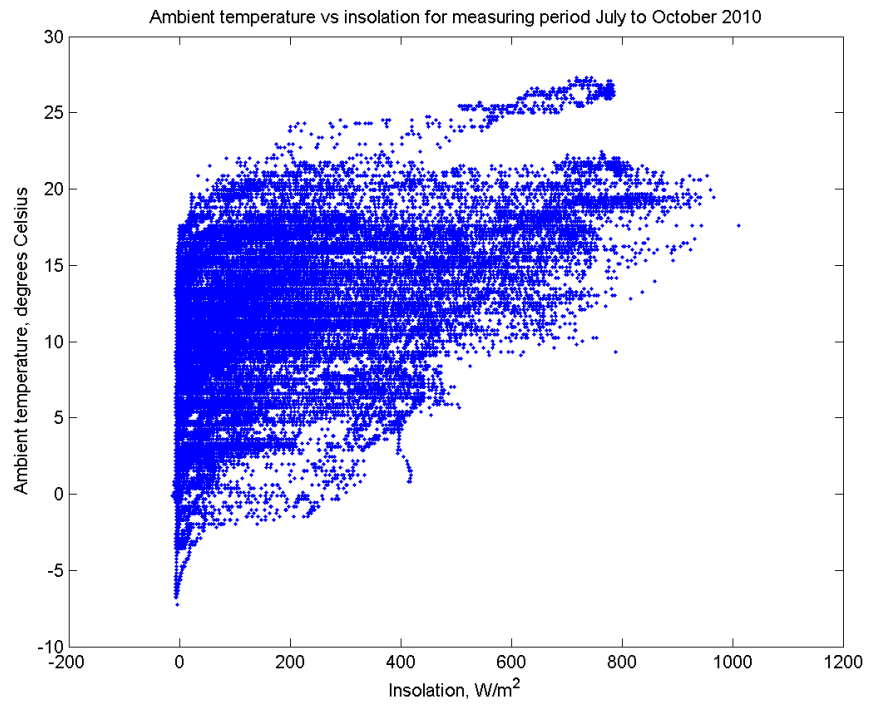


**Figure A1.5: Measured ambient temperature versus measured insolation for period July 2010 to October 2010**

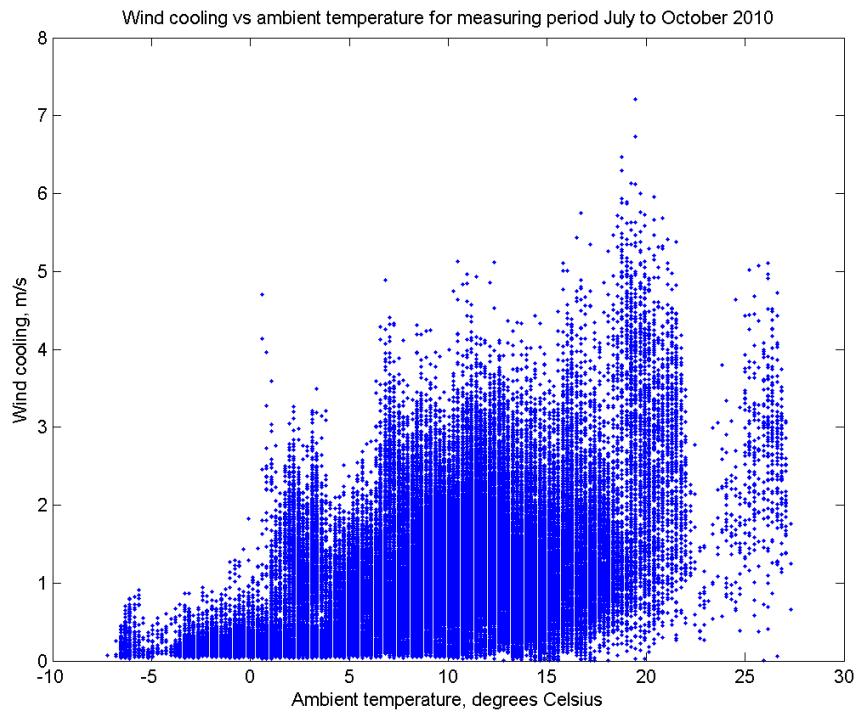


**Figure A1.6: Measured perpendicular wind versus measured insolation for period July 2010 to October 2010**

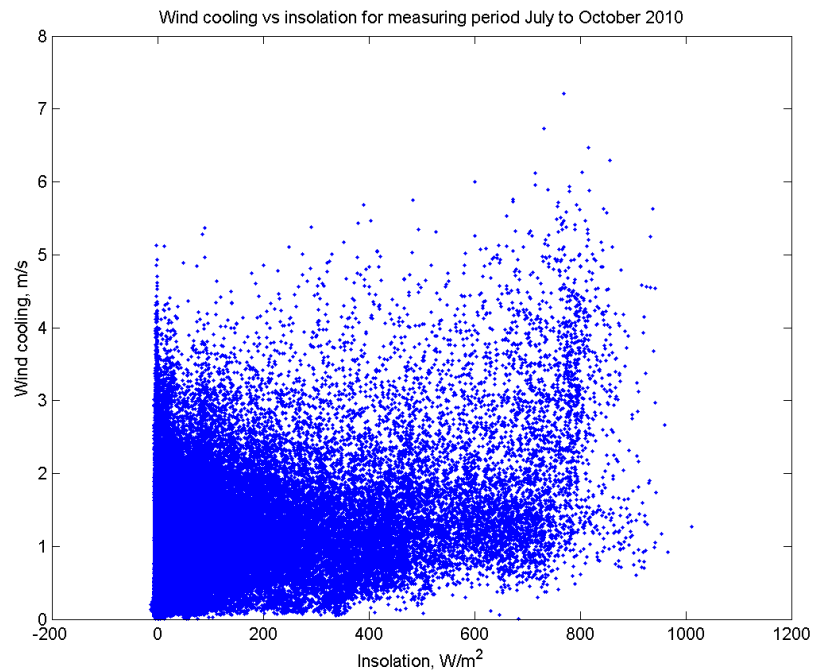


**Figure A1.7: Measured perpendicular wind versus measured insolation for period July 2010 to October 2010**

# Appendix 2

## Profile image for measured span on ZL8

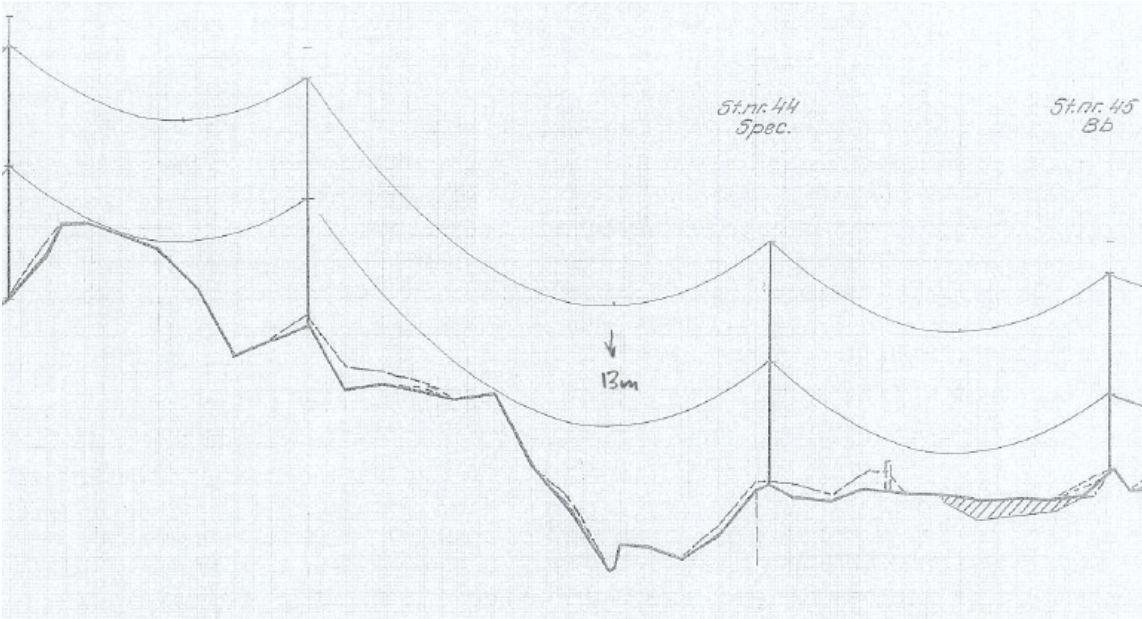
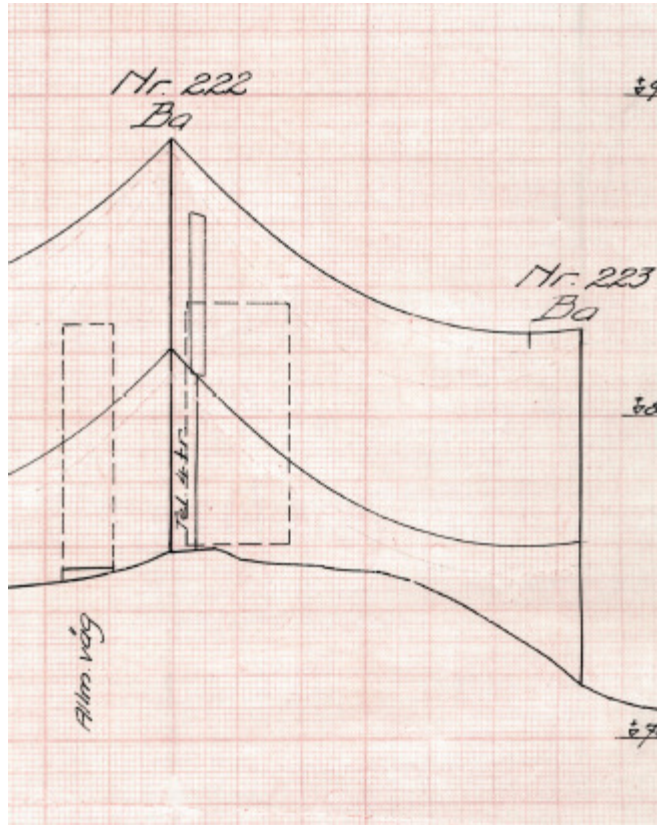


Figure A2.1: Profile image for measured span on ZL8. The span with measurement system is in the middle.

**Profile image for measured span on OL9**



**Figure A2.2: Profile image for measured span on OL9.**